Quantal puffs of intracellular Ca^{2+} evoked by inositol trisphosphate in *Xenopus* oocytes

Yong Yao, John Choi and Ian Parker*

Laboratory of Cellular and Molecular Neurobiology, Department of Psychobiology, University of California Irvine, CA 92717, USA

1. Ca^{2+} liberation induced in *Xenopus* oocytes by a poorly metabolized derivative of inositol 1,4,5-trisphosphate (3-deoxy-3-fluoro-D-*myo*-inositol 1,4,5-trisphosphate; 3-F-InsP_3) was visualized using a video-rate confocal microscope to image fluorescence signals reported by the indicator dye calcium green-1.

2. Low (10–30 nM) intracellular concentrations of 3-F-InsP_3 evoked Ca^{2+} release as localized transient 'puffs'. Progressively higher concentrations (30–60 nM) gave rise to abortive Ca^{2+} waves triggered by puffs, and then (> 60 nM) to a sustained elevation of Ca^{2+} followed by the appearance of propagating Ca^{2+} waves. At concentrations up to that giving waves, the frequency of puffs increased as about the third power of [InsP_3], whereas their amplitudes increased only slightly.

3. The rise of cytosolic Ca^{2+} during a puff began abruptly, and peaked within about 50 ms. The peak free Ca^{2+} level was about 180 nM, and the total amount of Ca^{2+} liberated was several attomoles (10^{-18} mol), too much to be accounted for by opening of a single InsP_3-gated channel. The subsequent decline of Ca^{2+} occurred over a few hundred milliseconds, determined largely by diffusion of Ca^{2+} away from the release site, rather than by resequestration. Lateral spread of Ca^{2+} was restricted to a few micrometres, consistent with an effective diffusion coefficient for Ca^{2+} ions of about 27 $\mu m^2 s^{-1}$.

4. The peak amplitudes of puffs recorded at a given site were distributed in a roughly Gaussian manner, and a small proportion of sites consistently gave puffs much larger than the main population. Intervals between successive puffs at a single site were exponentially distributed, except for a progressive fall-off in puffs seen at intervals shorter than about 10 s. Thus, triggering of puffs appeared to be stochastically determined after recovery from a refractory period.

5. There was little correlation between the occurrence of puffs at sites more than a few micrometres apart, indicating that puff sites can function autonomously, but closely (*ca* 2 μm) adjacent sites showed highly correlated behaviour.

6. Puffs arose from sites present at a density of about 1 per 30 μm^2 in the animal hemisphere, located within a narrow band about 5–7 μm below the plasma membrane.

7. We conclude that Ca^{2+} puffs represent a 'quantal' unit of InsP_3-evoked Ca^{2+} liberation, which may arise because local regenerative feedback by cytosolic Ca^{2+} ions causes the concerted opening of several closely clustered InsP_3 receptor channels.

Inositol 1,4,5-trisphosphate (InsP_3) is a second messenger that controls many cellular processes by inducing liberation into the cytosol of Ca^{2+} ions sequestered within intracellular organelles (Berridge, 1993). The characteristics of Ca^{2+} liberation are complex, and lead to the generation of repetitive Ca^{2+} spikes and propagating Ca^{2+} waves (Meyer & Stryer, 1991; Meyer, 1991; Berridge, 1993). *Xenopus* oocytes provide a favourable cell system in which to study these spatiotemporal aspects of InsP_3-mediated Ca^{2+} signalling, since their large size (> 1 mm diameter) both facilitates many experimental procedures, and offers a large 'playing field' on which to observe the spatial

* To whom correspondence should be addressed.

distribution of Ca^{2+} liberation. Imaging of oocytes loaded with fluorescent Ca^{2+} indicator dyes has revealed that stimulation by Ca^{2+}-mobilizing agonists and by direct introduction of $InsP_3$ into the cell leads to the generation of complex patterns of circular and spiral Ca^{2+} waves, which originate at particular foci and undergo mutual annihilation as they expand and crash into one another (Lechleiter, Girard, Peralta & Clapham, 1991; Parker & Yao, 1991; Lechleiter & Clapham, 1992; Yao & Parker, 1994). The oocyte cytoplasm thus behaves as an excitable medium, composed of stores that release their contents in a regenerative manner (Parker & Ivorra, 1990*a*, 1993), and which are coupled by the diffusion of a common stimulatory signal (Lechleiter & Clapham, 1992; Atri, Amundson, Clapham & Sneyd, 1993).

However, there is already evidence that the cytoplasm of the oocyte does not act as a uniform excitable medium, comprised of densely packed homogeneous Ca^{2+} stores. At a macroscopic level, the vegetal hemisphere is less sensitive to $InsP_3$ than is the animal hemisphere (Berridge, 1988). Microscopically, $InsP_3$ is seen to liberate Ca^{2+} at discrete sites, spaced several micrometres apart (Parker & Yao, 1991). Indeed, at low concentrations of $InsP_3$, Ca^{2+} liberation occurs at certain sites as transient 'puffs', that remain localized to within a few micrometres and fail to trigger propagating Ca^{2+} waves (Parker & Yao, 1991). The importance of these sensitive hot spots for cell functioning may be that they serve as pacemakers, acting as foci to generate Ca^{2+} waves and hence entrain neighbouring areas of the cell when levels of $InsP_3$ or basal intracellular Ca^{2+} are raised (Yao & Parker, 1994). Also, since the puff appears to represent a quantal unit of $InsP_3$-mediated Ca^{2+} liberation, it may provide information about both the physical arrangement of Ca^{2+} stores and the mechanisms underlying Ca^{2+} release.

The present paper describes a detailed characterization of Ca^{2+} puffs in *Xenopus* oocytes. Our main experimental approach was to inject oocytes with a poorly metabolized analogue of $InsP_3$, so as to evoke puff activity at a stable rate that was sustained for many minutes. Cytosolic free Ca^{2+} was then visualized using a high-affinity fluorescent indicator, calcium green-1. To optimize spatial resolution, a confocal microscope was used to obtain images from only a thin optical section at selected depths into the cell, while rejecting resting and Ca^{2+}-evoked fluorescence from regions above and below the plane of focus. In addition, a fast time resolution was required, since Ca^{2+} puffs last only a few hundred milliseconds (Parker & Yao, 1991). Most commercially available confocal microscopes were, therefore, unsuitable for our purpose, as they require a second or more to scan a single image field. Instead, we employed a 'real time' confocal microscope (Noran Odyssey; see Methods), which allowed capture of frames at a maximum rate of 60 s^{-1}.

METHODS

Preparation of oocytes

Experiments were done on defolliculated immature oocytes from albino *Xenopus laevis*. These were obtained by surgical removal from frogs anaesthetized by placing them in a 0·17% aqueous solution of MS-222 (3-aminobenzoic acid ethyl ester) for 15 min; frogs were allowed to recover after surgery. Procedures for preparation of oocytes and intracellular microinjection were as described previously (Sumikawa, Parker & Miledi, 1989; Parker, 1992). Each oocyte was loaded about 30 min before recording with about 40 pmol of the fluorescent Ca^{2+} indicator calcium green-1, resulting in a final intracellular concentration of approximately 40 μM. A sustained activation of $InsP_3$ signalling was induced by injecting oocytes with the poorly metabolized $InsP_3$ analogue 3-F-$InsP_3$ (3-deoxy-3-fluoro-D-*myo*-inositol 1,4,5-trisphosphate) (Kozikowsky, Fauq, Askoy, Seewald & Powis, 1990; Yao & Parker, 1993, 1994). In other experiments, where flashes of UV light were used to photorelease $InsP_3$ within the cell, oocytes were loaded with 2–5 pmol caged $InsP_3$ (*myo*-inositol 1,4,5-trisphosphate, $P^{4(5)}$-1-(2-nitrophenyl)ethyl ester) (McCray & Trentham, 1989). The amounts of compounds injected into oocytes were estimated by measuring the diameter of fluid droplets expelled by pneumatic pressure pulses applied when the micropipette tip was raised in the air, and final intracellular concentrations were calculated assuming even distribution throughout a cytosolic volume of 1 μl. During recording, oocytes were continually superfused with frog Ringer solution (composition (mM): NaCl, 120; KCl, 2; $CaCl_2$, 1·8; Hepes, 5; at pH about 7·0) at room temperature.

Oocytes were placed in a small recording chamber (Warner Instruments, Hamden, CT, USA) mounted on the stage of an Olympus IMT2 inverted microscope. The base of the chamber was formed by a no. 1 coverslip, allowing optical imaging and stimulation of the underside of the oocyte as described below. All recordings were made from the animal hemisphere of the oocyte. Micromanipulators mounted on the microscope stage were used to insert injection pipettes. However, because the oocyte is virtually opaque, it was not possible to view these pipettes through the inverted microscope. Instead, the condenser of the microscope was removed, and a stereo microscope was mounted in its place to assist in placing micropipettes. For safety, the stereo microscope was fitted with a long-pass filter (Schott OG 550; Melles Griot, Irvine, CA, USA) blocking wavelengths shorter than 550 nm, to avoid inadvertent exposure to the laser beam directed through the inverted microscope.

Confocal imaging

Fluorescence imaging of intracellular free Ca^{2+} was achieved using an Odyssey real time laser-scanned confocal microscope (Noran Instruments, Middleton, WI, USA). This had the great advantage of providing a video-rate output signal (RS-170; 30 interlaced frames s^{-1}), thus providing much better temporal resolution than is possible with most other commercially available systems that scan only one, or a few, frames per second. In brief, the Odyssey works by raster scanning a laser spot across the specimen, utilizing an accousto-optic device (AOD) for rapid x scan, and a galvanometer-driven mirror for the y scan. The intensity of fluorescence emission is monitored at each position of the scanning laser spot by a photomultiplier placed behind a confocal aperture, and is encoded as a standard

video signal. The AOD allows a much faster scan rate than is possible in systems using a galvanometer mirror for x deflection. However, a drawback is that the AOD cannot be used to descan the emitted fluorescence light, since this is of a longer wavelength than the excitation light, and would be deflected to a different extent. Instead, the fluorescence emission is descanned only by the y deflection mirror, and the confocal aperture is arranged as a slit aligned along the x scan of the laser spot. The design of the instrument, therefore, represents a trade-off between speed and axial resolution; use of an AOD provides fast frame acquisition, but rejection of out-of-focus fluorescence by the slit aperture is not quite as good as with a pinhole aperture.

The Odyssey was interfaced to an Olympus IMT-2 inverted microscope through the phototube on the microscope trinocular head. Fluorescence excitation was by the 488 nm line of a 100 mW multi-line argon ion laser, and emission of the Ca^{2+} indicator dye was monitored at wavelengths longer than 510 nm. Recordings were obtained using a Nikon ×40 Fluor oil-immersion objective lens (numerical aperture 1·3). Control of magnification was possible using the ×1·5 coupler lens incorporated in the Olympus microscope, and by the computer-controlled zoom function of the Odyssey. A range of confocal slits with widths between 15 and 100 μm could be selected and aligned under computer control. Determination of the optimal slit width represented a compromise between axial resolution and brightness of the image. Narrow slits gave better axial resolution, at the expense of lower light throughput, and hence noisier images. In most cases we used the 100 μm slit.

Because the rising phase of puffs occurs within only a few tens of milliseconds, this process could not be fully resolved even when scanning at 60 frames s^{-1}. Instead, we used the x-line scan mode of the Odyssey, where a single line across the oocyte was repeatedly scanned by the laser spot every 64 μs. A puff site was first identified by imaging, and the microscope stage was then moved to bring this site directly under the position of the line scan. Each horizontal line of a de-interlaced video frame thus displayed the intensity profile along the scan line, and successive lines were obtained at time intervals of 64 μs, so that the vertical height of the frame corresponded to 15·36 ms (240 lines × 64 μs). Successive frames were then 'pasted' together by computer to obtain a longer time record, and shot noise was reduced by forming a compressed image in which each scan line represented the average of four successive scans.

Photorelease of $Ins P_3$

UV light for photolysis of caged $Ins P_3$ loaded into the oocyte was derived from the standard 100 W mercury arc epifluorescence unit fitted to the Olympus microscope. An electronically controlled shutter (Uniblitz; Vincent Associates, Rochester, NY, USA) mounted in front of the lamp housing allowed flashes of various durations to be delivered, and the light intensity was set by continuously variable opposing neutral density wedges. Wavelengths shorter than about 400 nm were selected by an Olympus UV filter cube. Nearly uniform irradiation throughout the imaging field was achieved by adjusting the epifluorescence system for optimal Kohler illumination.

Image capture and processing

The video signal from the Odyssey was recorded on videocassettes using a professional S-VHS recorder (Sony SVO-9500MD). Subsequent image processing and analysis was performed off-line using the MetaMorph software package (Universal Imaging Corp., West Chester, PA, USA), running on an IBM-compatible PC equipped with a Matrox LC video card. Video frames of 480 × 512 pixels were captured with 8 bit (256 grey level) resolution and, when maximum time resolution was desired, frames were de-interlaced to obtain 60 frames s^{-1} with a reduced vertical resolution of 240 lines. Figures showing Ca^{2+} images were derived after first subtracting an averaged image of background fluorescence recorded before stimulation, and were usually processed by low-pass spatial filtering to reduce noise. Increasing levels of Ca^{2+} (higher fluorescence) are depicted on a pseudocolour scale ranging from dark blue (no Ca^{2+} increase) to red (maximal increase). Because ratio measurements cannot be made with calcium green-1, most of the pseudocoloured images and measurements of fluorescence provide only a relative, not absolute, measure of free Ca^{2+} concentration. However, in some instances (Fig. 4), fluorescence signals were calibrated using a procedure described in Results. All numerical values in the text are given as the mean ± 1 S.E.M.

Measurements of Ca^{2+} fluorescence as a function of time were obtained using the brightness-over-time function within MetaMorph. Active puff sites were identified from the monitor screen, and a square region of interest (usually 10 × 10 pixels; 3 × 3 μm) was centred over a site. Measurements of fluorescence averaged over this area were then captured at 20 samples s^{-1}.

Materials

Caged $Ins P_3$ and 3-F-$Ins P_3$ were obtained from Calbiochem (La Jolla, CA, USA), and calcium green-1 was from Molecular Probes (Eugene, OR, USA). All other reagents were from Sigma Chemical Co. (St Louis, MO, USA).

RESULTS

Ca^{2+} puffs and waves induced by 3-F-$Ins P_3$

We have previously shown that just suprathreshold photorelease of $Ins P_3$ evoked transient release of localized Ca^{2+} puffs in the oocyte (Parker & Yao, 1991). However, it remained possible that these localized responses may have been artifactual, resulting because variations in transmittance of the photolysis light into the cell led to local variations in concentration of photoreleased $Ins P_3$. To test this point, oocytes were injected with a poorly metabolized $Ins P_3$ analogue, 3-F-$Ins P_3$ (Yao & Parker, 1993), which was expected to distribute uniformly throughout the cell.

Oocytes were preloaded with calcium green-1 about 30 min before beginning recording. A region on the underside of the oocyte was then imaged by the inverted confocal microscope while 3-F-$Ins P_3$ was injected through a micropipette inserted so that its tip lay approximately in the centre of the oocyte. Responses were first detected about 2 min after loading a bolus of 3-F-$Ins P_3$, presumably because of the time required for this compound to diffuse the ~0·5 mm distance between injection and recording

sites. Injection of about 30 fmol 3-F-InsP_3 (which would give a final intracellular concentration of about 30 nM if evenly distributed throughout the cell) caused Ca^{2+} release, occurring sporadically as localized Ca^{2+} puffs (Fig. 1*A*). These Ca^{2+} signals were transient, lasting only a few hundred milliseconds, and remained localized to within a few micrometres. Injection of a further 30 fmol 3-F-InsP_3 gave an increased frequency of puffs, and some of these triggered abortive Ca^{2+} waves, which spread over a few tens of micrometres before dying out (Fig. 1*B*). Finally, injection of yet another 30 fmol 3-F-InsP_3 resulted in an initial wave of Ca^{2+} that swept over the recording field and then persisted at a uniform elevated level for a few minutes (Fig. 1*C*). In many oocytes, the overall fluorescence signal then began to decline, and propagating waves of Ca^{2+} became visible. At first these waves were faint, and were superimposed on a high background Ca^{2+} level. Also, they originated at high frequency from multiple foci, giving rise to chaotic patterns as opposing waves collided with and annihilated each other. Later, as the basal Ca^{2+} returned towards the resting level, Ca^{2+} waves became more sharply defined, and originated at lower frequency from a limited number of foci. For example, Fig. 1*D* illustrates a wave recorded about 4 min after the record in Fig. 1*C*.

The transition from a uniform Ca^{2+} elevation (Fig. 1*C*) to Ca^{2+} waves superimposed on a low background Ca^{2+} level (Fig. 1*D*) is unlikely to have arisen because of a fall in concentration of 3-F-InsP_3 at the recording site. Indeed, the concentration probably continued to rise, due to diffusion from the injection site. It is also unlikely that metabolism of 3-F-InsP_3 would have contributed to the change in pattern of Ca^{2+} release, since puffs evoked by injections of low concentrations of 3-F-InsP_3 persisted at a steady frequency for more than 20 min (see later). The decline in sustained Ca^{2+} liberation and appearance of waves may, therefore, result from a partial desensitization or adaptation of the InsP_3 receptors in the face of a maintained high concentration of agonist.

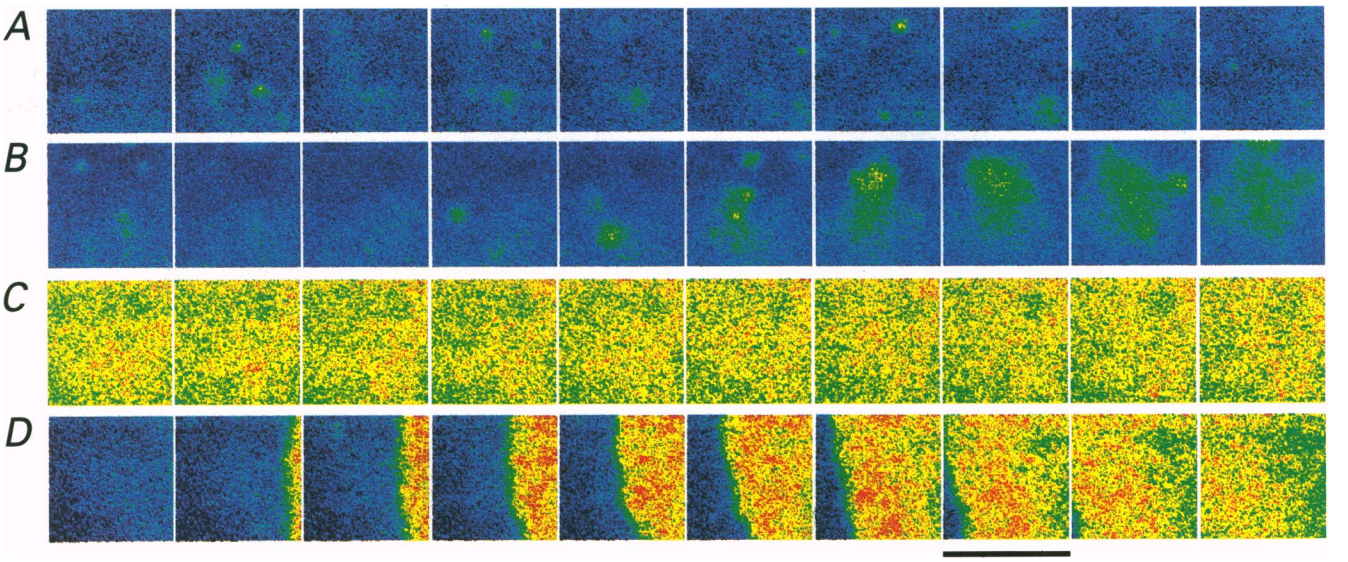

Figure 1. Pseudocoloured images showing different patterns of Ca^{2+} liberation induced by various concentrations of 3-F-InsP_3

Images were obtained from a fixed region (70 × 70 μm) of a single oocyte, and frames within each row were captured at 1 s intervals. The oocyte was loaded with calcium green-1 (final intracellular concentration 30 μM), and increasingly 'warm' colours represent progressively increasing levels of Ca^{2+}-dependent fluorescence above the resting level seen before injecting 3-F-InsP_3. The magnitude of Ca^{2+} changes is uncalibrated, but the pseudocolour scale is consistent for all frames in the figure. Images were low-pass filtered using a 3 × 3 pixel (0·8 × 0·8 μm) window, and are an average of 3 consecutive interlaced video frames. *A*, images obtained 9 min after injecting 30 fmol 3-F-InsP_3 to attain a final intracellular concentration of about 30 nM. Ca^{2+} release was apparent as localized puffs (yellow spots), which were transient and failed to spread more than a few micrometres. *B*, image sequence 3 min after loading an additional 30 fmol 3-F-InsP_3. Some puffs now gave rise to abortive Ca^{2+} waves, which spread more extensively (a few tens of micrometres), and persisted for a few seconds. *C*, 2 min after injecting a further 30 fmol 3-F-InsP_3 the intracellular Ca^{2+} became uniformly elevated throughout the recording field for several minutes. Thereafter, the overall Ca^{2+} level declined, and Ca^{2+} waves then became evident (*D*). Scale bar, 70 μm.

Results like those in Fig. 1 were seen in more than thirty oocytes examined, and Fig. 2 summarizes the estimated cytosolic concentrations of 3-F-InsP_3 required to evoke the various patterns of Ca^{2+} liberation (puffs, abortive waves, propagating waves, and sustained elevation of Ca^{2+}). Measurements were made 5–10 min after injection to allow for diffusional equilibration throughout the cell. Puffs were detected at intracellular concentrations as low as 10 nM, and, because 3-F-InsP_3 is about equipotent to InsP_3 in releasing Ca^{2+} in Swiss 3T3 cells (Kozikowski *et al.* 1990), the concentration of endogenous InsP_3 required to evoke puffs is presumably similar. Since Ca^{2+} puffs were seen a long time (several hours) after injection and at appreciable distances (0·5 mm) from the site of injection, it is implausible that they could have arisen from locally high concentrations of 3-F-InsP_3. Also, we observed puffs in response to photoreleased InsP_3 (next section), and in oocytes ($n = 3$) which were exposed to lysophosphatidic acid in the bathing solution so as to generate endogenous InsP_3 by activation of membrane receptors (Tigyi & Miledi, 1992). Thus, the puffs did not arise through some peculiar action of 3-F-InsP_3, but, instead, almost certainly represent a physiological phenomenon.

Dose dependence of puffs

Because of the need to wait several minutes after injection of 3-F-InsP_3 for diffusional equilibration, it was difficult to use this technique for more quantitative studies of the dose dependence of puff activation. Instead, we loaded oocytes with caged InsP_3, and used flashes of UV light of varying intensity to photorelease differing amounts of InsP_3. The extent of photorelease was expected to be linearly proportional to flash duration (Parker & Ivorra, 1992), but the absolute concentration of InsP_3 resulting from each flash was unknown.

The photolysis light was arranged to illuminate the entire field (140 × 130 μm) viewed by the confocal microscope, and the numbers of puffs observed in this field during a 10 s period following each flash were counted by visual inspection of videotaped records. Puffs continued for about 40 s after each flash, a period which presumably corresponds to the time required for metabolic breakdown of the photoreleased InsP_3 and its diffusion out of the recording field. Flashes of increasing duration evoked progressively more puffs and, beyond a certain threshold duration, propagating waves were triggered. In order to pool data from differing areas of the cell we normalized the flash durations as a percentage of that required to evoke waves at each area. Figure 3*A* shows the dependence of puff frequency during the first 10 s after a flash as a function of stimulus strength (flash duration). This varied in a non-linear manner, with the puff frequency increasing as about the third power of the expected extent of InsP_3 liberation.

In contrast to the steep dependence of puff frequency on flash duration, the amplitude of puffs increased only

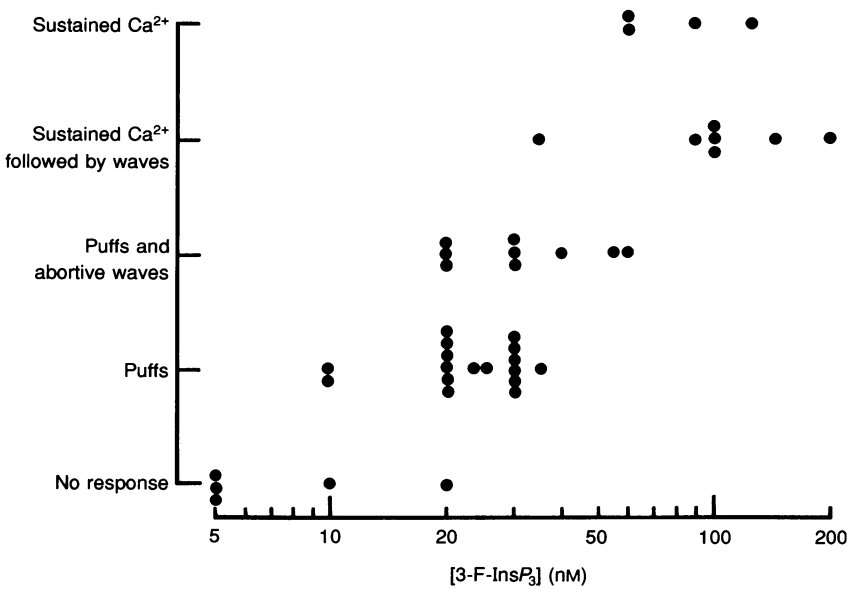

Figure 2. Patterns of Ca^{2+}-release activity as a function of 3-F-InsP_3 concentration

The figure summarizes data from 27 oocytes that were injected with 3-F-InsP_3 to varying final intracellular concentrations. Points indicate the pattern of release observed 5–10 min after each injection. Oocytes were considered to show sustained Ca^{2+} release if the fluorescence remained uniformly high for 5 min after injection. Those marked as showing sustained release plus waves showed an initial spatially uniform elevation lasting 2–3 min, followed by the appearance of waves as the overall Ca^{2+} level declined. No response means that we failed to observe even a single puff in the imaging field (140 × 130 μm) during a 5 min period.

slightly with increasing photorelease of InsP_3 (Fig. 3*B*). For example, increasing the flash duration from 50 to 100% of the wave threshold increased puff frequency about 8-fold, whereas the mean puff amplitude increased by less than 50%.

Calibration of fluorescence signals

Our confocal microscope is limited to excitation at visible wavelengths, and no currently available visible wavelength Ca^{2+} indicator dyes show spectral shifts that would allow ratiometric calibration of fluorescence signals in terms of absolute free Ca^{2+} concentration. We therefore calibrated puff signals by determining calcium green-1 fluorescence from the same regions of the oocyte in the virtual absence of free Ca^{2+} (F_{min}), and in the presence of saturating Ca^{2+} (F_{max}). The free Ca^{2+} concentration corresponding to any particular fluorescence level, F, is then given by:

$$[Ca^{2+}] = K_d(F - F_{min}) / (F_{max} - F), \quad (1)$$

where K_d is the dissociation constant for the indicator, determined as 247 ± 15 nM (3 replicates) using a calcium calibration buffer kit with solutions including 100 mM KCl and 1 mM $MgCl_2$ (Calcium Calibration Buffer Kit C3722; Molecular Probes Inc.).

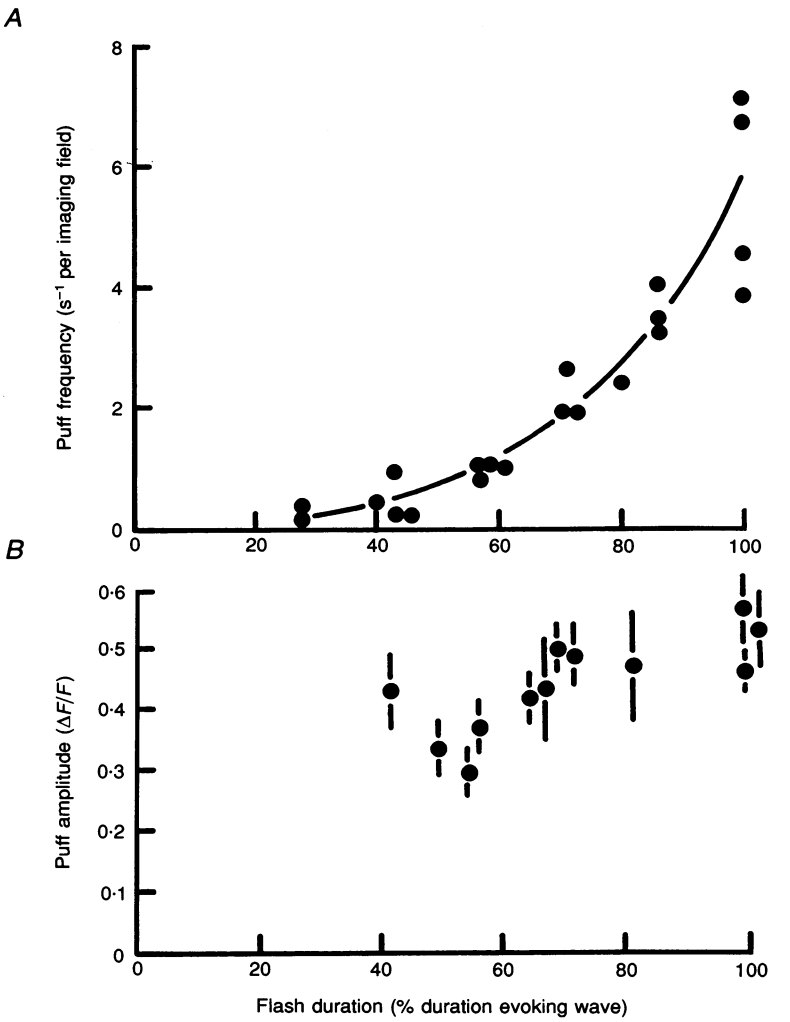

Figure 3. Dose dependence of puff activation studied by flash photolysis of caged InsP_3

Data were obtained from 5 regions of a single oocyte that was loaded with 2·4 pmol caged InsP_3 together with calcium green-1. Brief (< 70 ms) photolysis flashes of varying duration were applied to photorelease various amounts of InsP_3 uniformly across the imaging field. Flash durations are normalized as a percentage of that duration which just evoked a Ca^{2+} wave at each imaging region. *A*, dependence of puff frequency on duration of photolysis flash. Puff frequencies were determined by counting the number of puffs observed within 10 s following a flash or, in the case of flashes that evoked Ca^{2+} waves, the number of puffs observed in the time (1–2 s) before a wave was initiated. The curve shows a 3·1-power relationship fitted to the data. *B*, dependence of puff amplitude on flash duration. Measurements show peak fluorescence intensities ($\Delta F/F$) measured over 5 × 5 μm measuring boxes positioned over puff sites. Points indicate means ± S.E.M. of measurements from 3 to 9 sites in each trial.

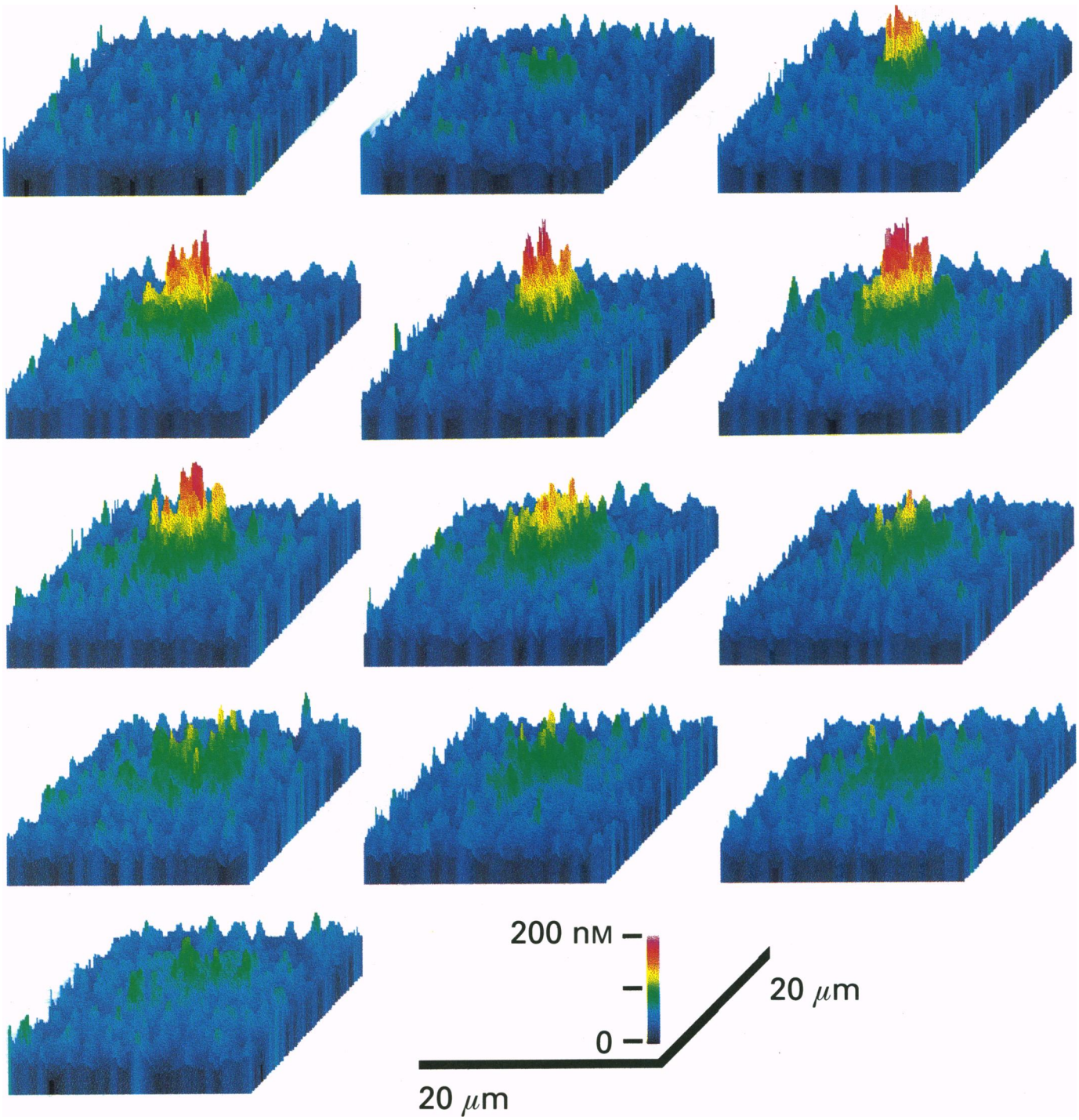

Figure 4. High resolution images showing a Ca^{2+} puff evoked by photoreleased InsP_3

Successive frames (left to right, top to bottom) were captured at intervals of 16·67 ms by de-interlacing odd and even scans of the video signal from the confocal microscope. Each frame corresponds to a 20 × 20 μm region of the oocyte, and the plane of the confocal section was located at a depth of about 5 μm into the oocyte. Digitized images were smoothed by a 7 × 7 pixel (0·6 × 0·6 μm) low-pass filter. Increasing intracellular free Ca^{2+} concentrations are depicted by increasingly 'warm' colours, and by increasing the height of the line associated with each pixel. The colour bar indicates Ca^{2+} concentrations (in nM) on a linear scale, and was calibrated as described in the text. The oocyte was loaded with about 40 pmol calcium green-1 together with 2 pmol caged InsP_3.

Measurements of peak fluorescence of puffs were made in oocytes loaded with calcium green-1 and caged $InsP_3$. First, puffs were evoked by delivering relatively weak photolysis flashes. A strong photolysis flash was then applied to cause a massive liberation of intracellular Ca^{2+}. The resulting cytosolic free Ca^{2+} level was sufficient to virtually saturate the indicator dye, as demonstrated in control experiments where flash-evoked fluorescence signals were compared to those evoked by microinjection of saturating amounts of Ca^{2+} into the cell. Finally, a pipette filled with 1 M EGTA was inserted into the oocyte, and F_{min} was estimated 5 min after loading the cell to a final intracellular concentration of about 20 mM EGTA.

The mean ratio F_{max}/F_{min} determined in this way in ten oocytes was $3{\cdot}9 \pm 0{\cdot}2$. This value was only about one-third of that measured in calibration solutions ($12{\cdot}2 \pm 0{\cdot}8$), possibly as a result of Ca^{2+}-insensitive fluorescence of dye immobilized or compartmentalized in the oocyte (cf. Parker & Ivorra, 1993). Using *in vivo* measurements of F_{min} and F_{max}, together with a dissociation constant of 247 nM, the resting free cytosolic Ca^{2+} concentration was estimated to be 39 ± 4 nM ($n = 10$). Measurements of ten puffs indicated that the mean peak free Ca^{2+} was 180 ± 20 nM, i.e. an increase of about 140 nM above the resting level. These values are, however, only approximate, and do not take into account any changes in properties of the indicator that may result in the cell from factors including differences in ionic strength from the calibrating solution, viscosity and presence of proteins.

Time course and spatial spread of Ca^{2+} during a puff

Figure 4 shows high resolution images illustrating the appearance of a puff within a 20×20 μm region of an oocyte. Increasing Ca^{2+} levels are depicted by a pseudocoloured three-dimensional plot, in which the vertical height and colour of each pixel are proportional to the free Ca^{2+} concentration. Calibration of the fluorescence intensity of each pixel in terms of nanomolar concentrations of free Ca^{2+} was achieved by the procedure described above, using images of the same recording area in the presence of saturating Ca^{2+} and after loading EGTA. The plane of the confocal section was focused about 5 μm into the oocyte because, as described later, this gave the sharpest resolution of the initial Ca^{2+} release. Also, the video frames recorded on S-VHS tape were de-interlaced after digitization, to provide temporal resolution of 60 images s^{-1}.

Ca^{2+} release was first visible during the second frame of Fig. 4, and the peak Ca^{2+} level was attained three or four frames (50–67 ms) later. At this time Ca^{2+} was elevated within a region of about 6 μm diameter, and the signal then became progressively fainter and more diffuse, until it could no longer be clearly discerned above the background noise after about twenty frames (333 ms). Within the limit of our resolution, it appeared that the distribution of cytosolic Ca^{2+} was consistent with Ca^{2+} ions diffusing from a point source of release, rather than being released over an appreciable area or from multiple closely spaced sites. Although several 'peaklets' are evident in the images in Fig. 4; these probably arose from noise fluctuations in the recording. The positions of the peaklets were not consistent from one frame to the next, as would be expected if they represented discrete release sites, and random noise peaks of similar size were evident in the background signal away from the puff site.

Measurements of Ca^{2+} kinetics during a puff were made by recording fluorescence from a small (3×3 μm) region of interest centred on puff release sites. Figure 5*A* shows a record formed by averaging eighteen puffs occurring at a single site so as to reduce noise fluctuations. Several features are evident. Firstly, puffs began abruptly from a steady baseline, without any detectable evidence of a preceding pacemaker rise in Ca^{2+} level (Parker & Yao, 1991). The rise in cytosolic Ca^{2+} to the peak was then rapid, and could not be adequately resolved in recordings at video frame rate (30 s^{-1}). Finally, the Ca^{2+} level declined over a roughly exponential time course, with a time constant of about 250 ms for the record of Fig. 5*A*.

The major factor determining the decline of puffs was diffusion of Ca^{2+} ions away from their localized site of origin, rather than their removal from the cytosol by resequestration. This is illustrated in Fig. 5*B*, which compares normalized, averaged fluorescence signals recorded from a restricted region (3×3 μm) centred on a puff site (rapidly declining trace) and from a wider (10×10 μm) concentric region (more slowly declining trace). The local signal at the puff site fell to one-half of its peak value within about 100 ms. In contrast, the signal obtained from a wide area, which includes contributions from Ca^{2+} ions diffusing laterally away from the release site, showed a decay half-time of about 375 ms. Furthermore, even this relatively slow decay could largely be accounted for by axial diffusion of Ca^{2+} out of the plane of the confocal section. The dashed lines in Fig. 5*B* were calculated assuming that Ca^{2+} ions diffused with a coefficient of 25 μm^2 s^{-1} (see later) from a point source in the middle of a confocal slice 5 μm thick, and provide a good fit to the data. In agreement with this interpretation, fluorescence signals evoked by photorelease of $InsP_3$ over relatively wide areas to minimize diffusional loss of Ca^{2+} decayed with a half-time of about 2 s (Parker & Ivorra, 1993), indicating that Ca^{2+} sequestration cannot be faster than this.

Line scan imaging of puffs

As noted above, Ca^{2+} transients during puffs were so rapid as to be only poorly resolved by standard video microscopy. Also, resolution of the spatial spread of Ca^{2+} was poor, because of appreciable shot noise fluctuations in single frames. To overcome these limitations, we imaged puffs using the line scan mode of the confocal microscope. This involved repeatedly scanning the laser spot along a single line every 64 μs. Although spatial information was then restricted to a single dimension, temporal resolution

was enormously enhanced, and in practice was partly traded off for an improvement in the signal-to-noise ratio by averaging over several successive scans. The kinetics of the indicator dye would not have significantly limited time resolution. The on and off rates for binding of Ca^{2+} to calcium green-1 are, respectively, about 6×10^8 M^{-1} s^{-1} and 200 s^{-1} at room temperature and neutral pH (Eberhard & Erne, 1991), so that the fluorescence signal should have tracked Ca^{2+} signals during a puff with negligible lag.

Figure 6*B* and *E* shows line scan images of a single puff. Ca^{2+} concentration is encoded by colour; the vertical axis represents position along the scan line, and time runs horizontally. Other traces in the figure show measurements derived from these images, including time-dependent changes in Ca^{2+} fluorescence at the centre of the puff site (Fig. 6*A* and *D*), and representative profiles of Ca^{2+} distribution along the scan line at various times (Fig. 6*C* and *F*). Ca^{2+} release began within a region less than 1 μm across, which was about the limit of our resolution. Furthermore, the subsequent rise and spread of Ca^{2+} appeared consistent with diffusion from a virtual point source, and we did not see evidence of release from multiple discrete sources (6 puff events examined). The Ca^{2+} level at the release site in Fig. 6 continued to rise for about 50 ms, and similar values (40–57 ms) were found in recordings of five other puffs. This, therefore, provides an indication of

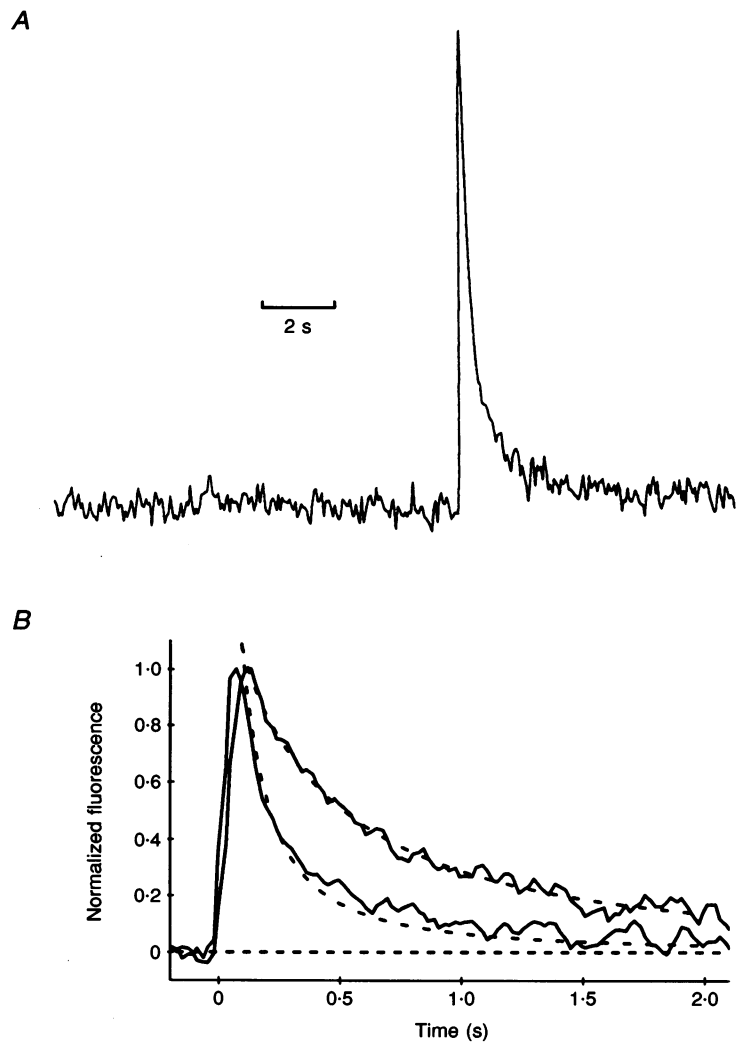

Figure 5. Kinetics of Ca^{2+} during a puff

A, measurements of Ca^{2+}-dependent fluorescence obtained at a 20 Hz sampling rate from a 10 × 10 pixel (3 × 3 μm) region of interest centred on a puff site. To reduce noise, traces derived from 18 separate puff events at the same site were averaged after aligning so that their peaks coincided. *B*, decay of Ca^{2+} at a puff site is determined largely by diffusion and not by resequestration of Ca^{2+}. Traces show averaged fluorescence signals measured from 13 puffs at different sites using a small (3 μm square) region of interest centred over the puff site (lower trace) and a larger (10 μm square) concentric region (upper trace). The traces were normalized to the same peak amplitude to facilitate comparison of decay rates. Dashed curves were derived by computer simulation of Ca^{2+} diffusion from a point source, assuming a confocal section 5 μm thick and a diffusion coefficient of 25 μm^2 s^{-1}.

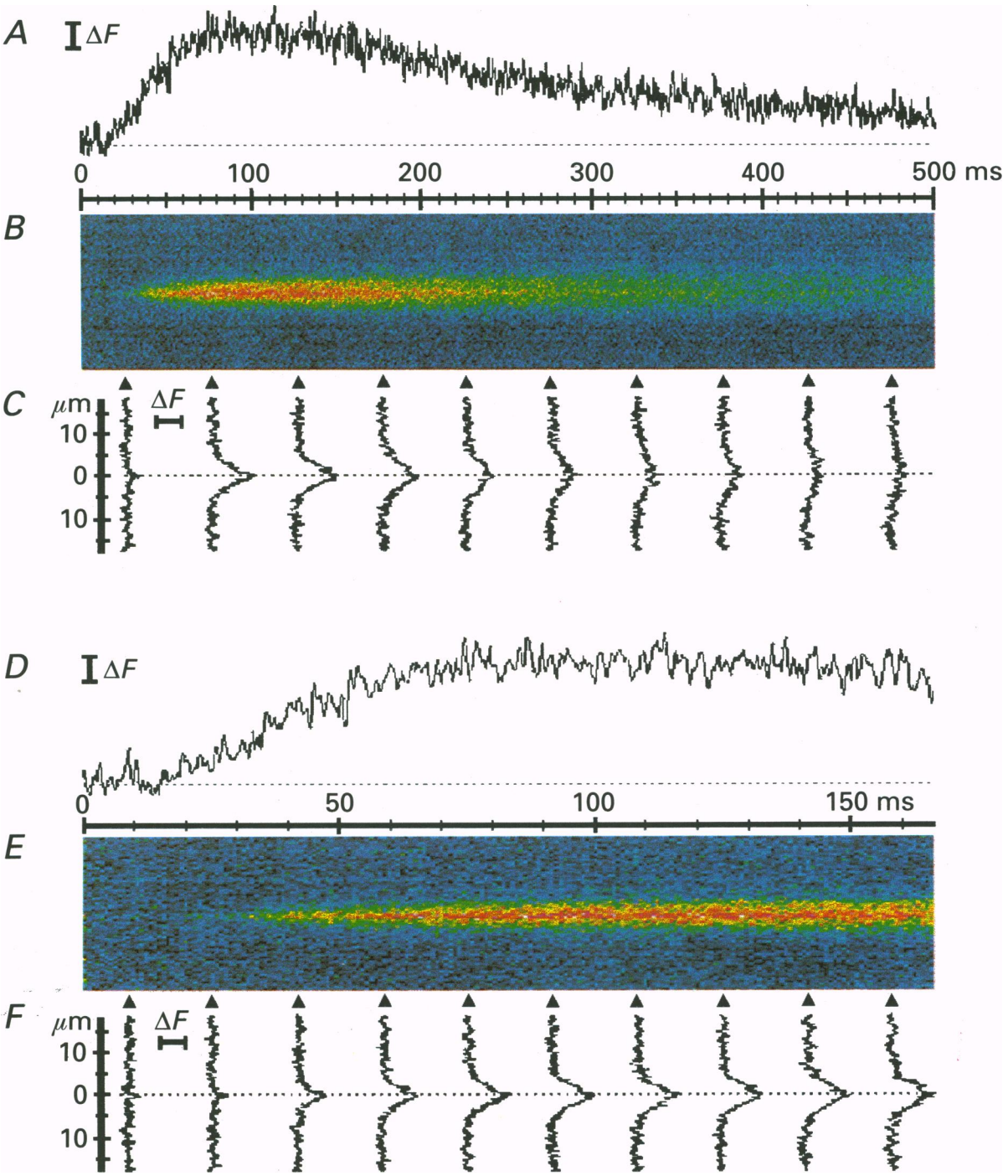

Figure 6. Recording of a puff with increased temporal resolution using the line scan mode of the confocal microscope

The images in *B* and *E* were obtained by repeatedly scanning the laser spot along a single line centred on a puff site at a 64 μs repetition rate. Time is displayed running horizontally along the image, and distance along the scanned line (total length 35 μm) runs from top to bottom. See Methods for further details. *A*, kinetics of the puff derived by recording fluorescence intensity within a 15 pixel (1 μm) section of the line scan at the centre of the puff. The trace was smoothed by a moving average over a 1·3 ms window. The calibration bar (ΔF) represents 5 grey scale intensity units. *B*, pseudocoloured line scan image of a single puff. Time is indicated by the horizontal scale, and the vertical distance scale in (*C*) applies also to the image. Increasingly 'warm' colours denote increasing Ca^{2+}-dependent fluorescence above the resting level, but are not calibrated in terms of absolute free Ca^{2+} concentration. *C*, representative traces showing the distribution of Ca^{2+}-dependent fluorescence along the line scan at various times as marked by the arrowheads. Each trace was obtained by smoothing over 84 successive scan lines (5·4 ms). The calibration bar (ΔF) represents 15 intensity units. *D*, *E* and *F*, the same data presented on an expanded time scale to display better the rise of the puff.

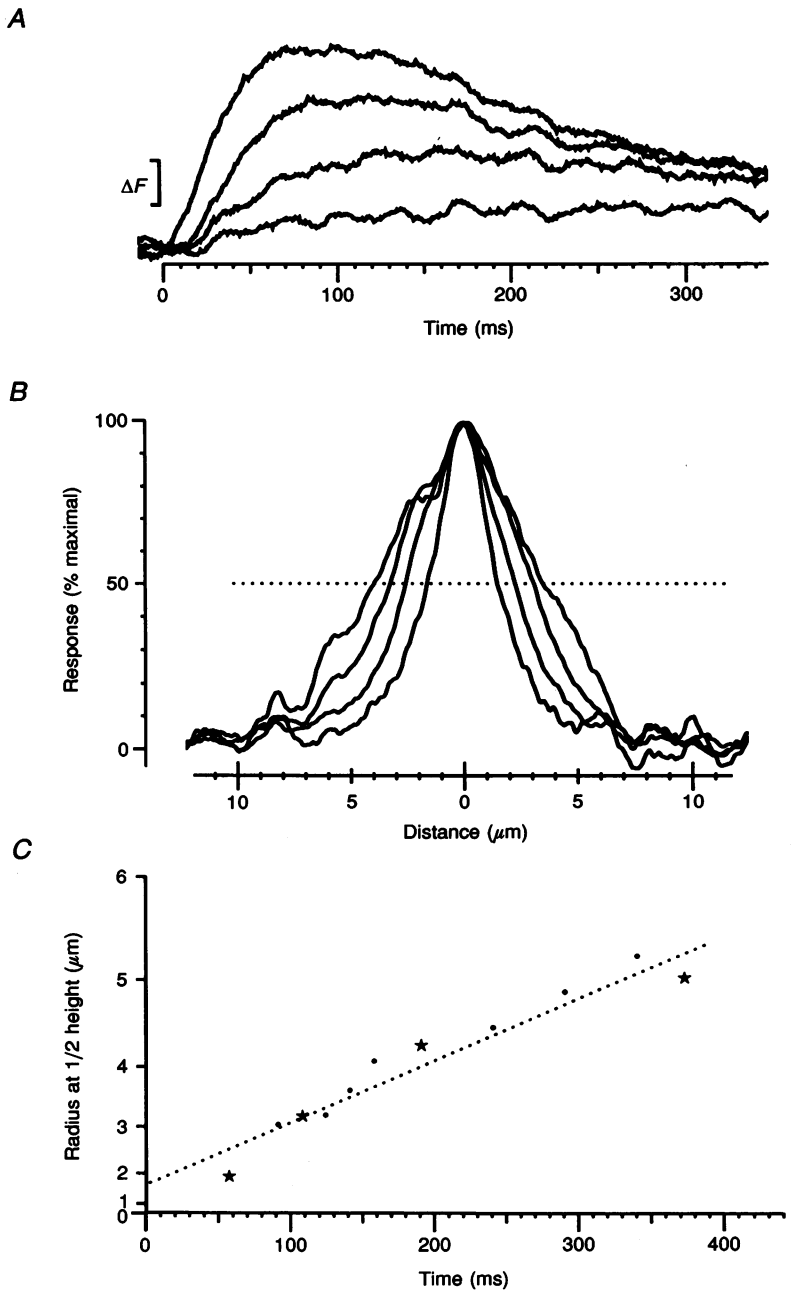

Figure 7. Spatial spread of Ca^{2+} from a puff site and estimation of diffusion coefficient for Ca^{2+} ions in the cytosol

A, superimposed traces showing Ca^{2+}-fluorescence signals recorded at distances of 0, 2, 3·4 and 5·4 μm from the centre of the puff site illustrated in Fig. 6. The signals became progressively smaller and slower with increasing displacement from the puff site. Traces were obtained by averaging fluorescence across a 15 pixel (1 μm) wide strip along the line scan image and smoothing over a 21 ms time window. Calibration bar corresponds to a ΔF value of 5 intensity units. *B*, superimposed traces show distributions of Ca^{2+} fluorescence along the scan line at times of about 60, 110, 190 and 375 ms after the beginning of a puff. The spread of Ca^{2+} increased progressively with time, and the amplitudes of the traces were normalized to the same peak value. Records at 60 and 110 ms were obtained by averaging 41 successive scan lines (2·6 ms), and those at later times were averaged over 81 scan lines and smoothed over a 1·4 μm running window to compensate for the increased noise level after normalization. Data are from the same event as Fig. 6. *C*, graph shows width of the Ca^{2+}-fluorescence signal as a function of time. Points marked by ★ correspond to the traces illustrated in *B*. Note that the vertical axis is scaled as distance squared. A regression line is drawn through the data.

the duration of Ca^{2+} liberation giving rise to a puff. At the time of the peak Ca^{2+} level, Ca^{2+} was restricted to within about a 4 μm radius of the release site. Subsequently, the Ca^{2+} level at the centre declined with a half-time of about 200 ms, and became more diffusely distributed.

The traces in Fig. 7*A* provide an indication of Ca^{2+} signals monitored at different displacements from a puff release site. As expected from diffusion of Ca^{2+} arising at a virtual point source, Ca^{2+} signals at progressively greater distances began after increasing latencies, attained lower peak amplitudes, and became more sluggish in their rise and fall. A useful measure of the range of action of Ca^{2+} ions (cf. Allbritton, Meyer & Stryer, 1992) is the effective space constant of a puff, defined as the radial distance at which the peak Ca^{2+} level attained is 1/e of the peak level directly at the release site. For the puff in Figs 6 and 7*A* this was about 3·1 μm, and similar measurements of five other puffs gave a mean value of 2·8 $\pm$ 0·25 μm.

Estimation of effective diffusion coefficient for Ca^{2+} in the cytosol

Puffs provide a favourable and simple situation in which to study diffusion of Ca^{2+} within an intact cell, since a certain quantity of Ca^{2+} is deposited into the cytosol at a virtual point source within a relatively short (50 ms) time. To derive an estimate of the effective diffusion coefficient determining spread of Ca^{2+} during a puff, we took traces of Ca^{2+} distribution like those in Fig. 6*C*, and normalized them to the same peak amplitude (Fig. 7*B*). Measurements were then taken at various times of the width of the Ca^{2+} distribution at half of the peak amplitude. Figure 7*C* shows a plot of the corresponding radii (r) as a function of time (t). From Fick's law, r is expected to increase proportional to the square root of t, and a good fit to a straight line was obtained by plotting r^2 against t (Fig. 7*C*). Effects of Ca^{2+} sequestration were cancelled out by the normalization procedure, and in any case the measuring period (400 ms) was short compared with the rate of Ca^{2+} uptake (half-time

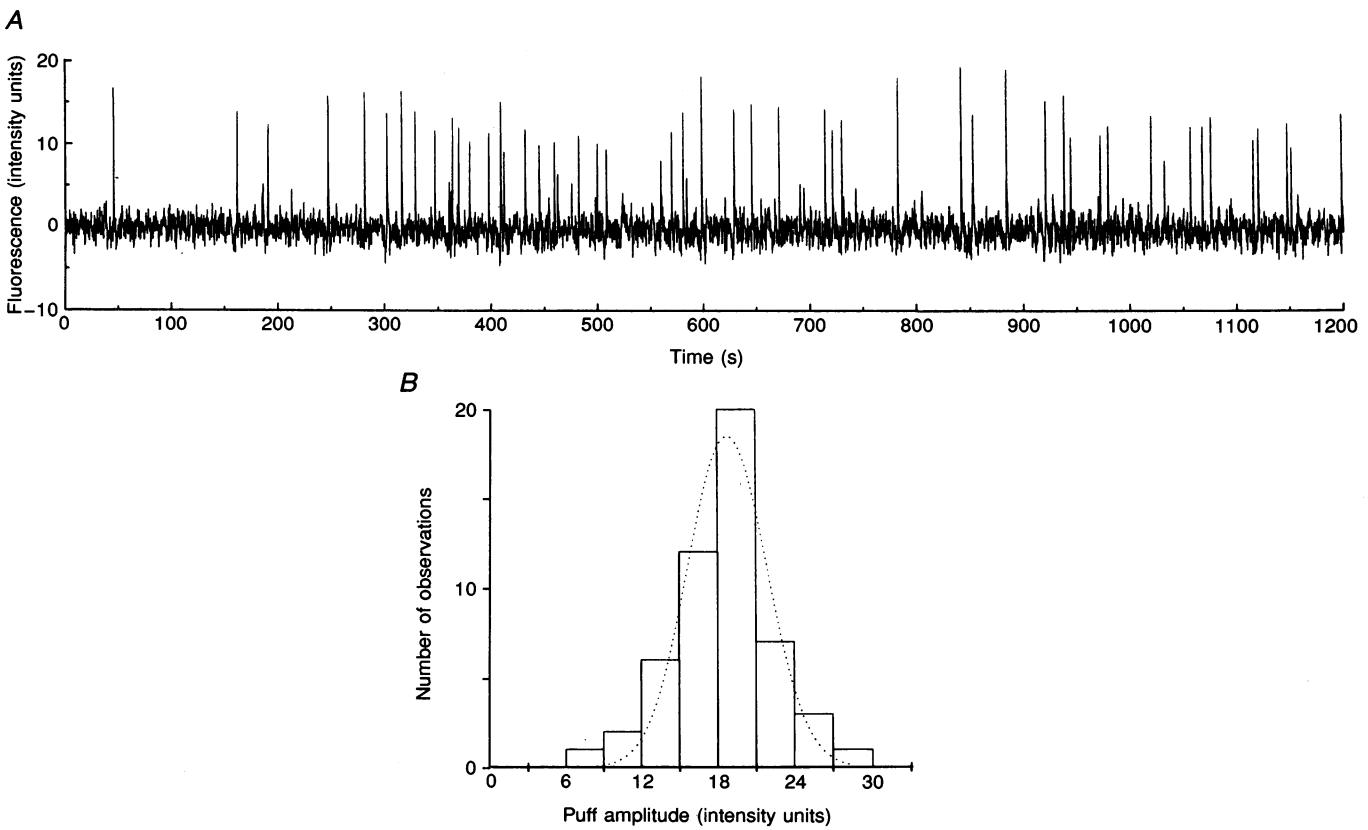

Figure 8. Continuous record of puffs originating at a single site and distribution of puff amplitudes

A, trace shows fluorescence measurements (256 level grey scale) obtained at 50 ms intervals from a 3 × 3 μm region of interest centred on a puff site after subtracting a running average of background fluorescence intensity. The oocyte was loaded with 25 fmol 3-F-InsP_3 and 40 pmol calcium green-1. *B*, distribution of puff amplitudes derived from the trace in *A*. Events smaller than 6 intensity units were not counted, so as to exclude noise spikes, and weak signals arising from Ca^{2+} diffusing from adjacent puff sites. Curve is a Gaussian distribution, with a mean of 18·8 intensity units and standard deviation 6·1 units.

> 2 s). The slope of the line in Fig. 7*C* could then be used to estimate the effective diffusion coefficient (D) for Ca^{2+} since (Crank, 1975):

$$C/C_0 = \exp(-r^2/4Dt), \quad (2)$$

where C/C_0 is the Ca^{2+} concentration at any given time normalized to the Ca^{2+} concentration at the centre of the puff at the same time. Then,

$$D = (\text{slope})/(-4\ln(C/C_0)). \quad (3)$$

For the puff in Figs 6 and 7, D was estimated to be about 24 $\mu m^2\ s^{-1}$, and a mean value of $27 \pm 4\ \mu m^2\ s^{-1}$ was obtained from analysis of six puffs. Because this value was derived from measurements made using 40 μM calcium green-1, it may overestimate the physiological diffusion coefficient due to the presence of exogenous, mobile Ca^{2+} buffer, but will be applicable to other recordings made under similar experimental conditions. Also, the diffusion coefficient varies with free Ca^{2+} concentration (Allbritton *et al.* 1992), and would probably be greater for the higher free Ca^{2+} concentrations attained during Ca^{2+} waves.

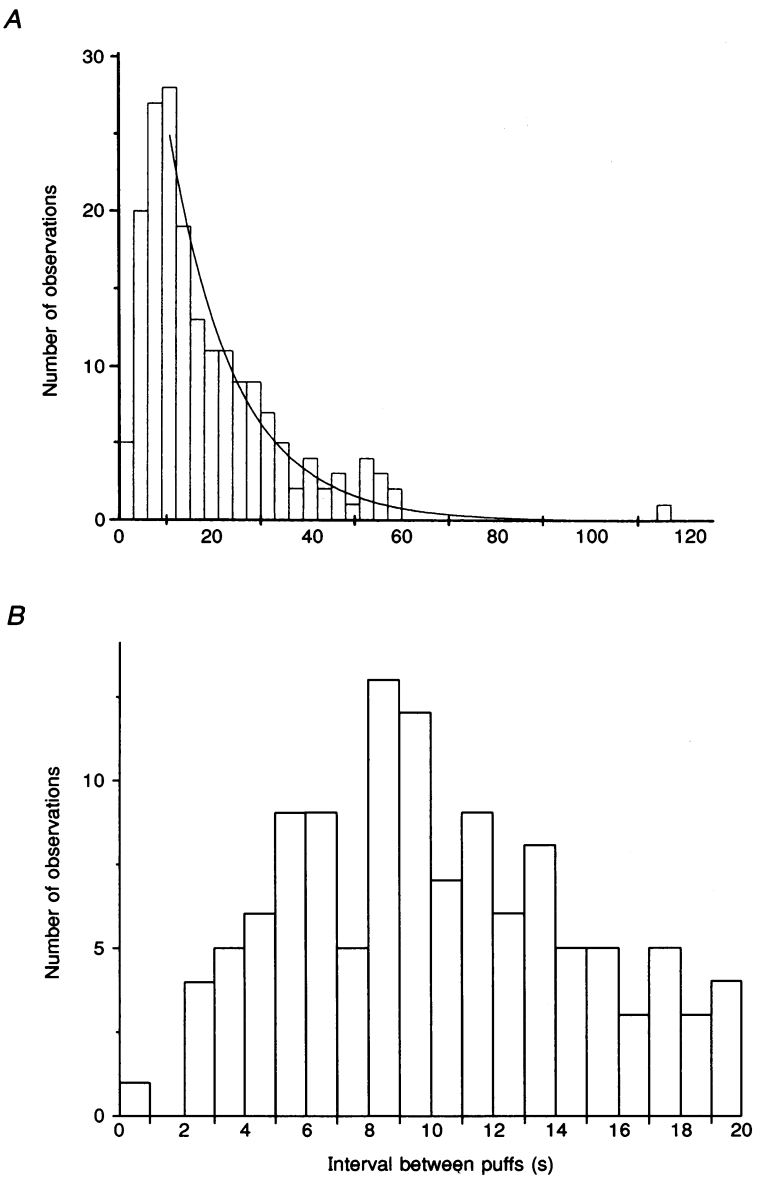

Figure 9. Distribution of intervals between successive puffs at individual sites

Pooled data are shown from 3 puff sites, which showed mean intervals between 9·3 and 15·2 s. *A*, distribution of all 186 events recorded. The curve is an exponential with a time constant of 14 s fitted to measurements at intervals longer than 10 s. *B*, same data as in *A*, but re-binned and plotted on an expanded time scale to illustrate better the fall-off in occurrence of puffs at intervals shorter than about 8 s.

Amplitude distribution of puffs

Recordings of fluorescence from individual puff sites showed that successive puffs tended to be of roughly similar size. For example, Fig. 8*A* shows a continuous record lasting 20 min obtained from a single puff site. There was no evidence for any systematic change in puff amplitude throughout this period, and the mean amplitudes of the first and last twenty-five puffs were 18·6 ± 3·8 and 19·0 ± 3·8 intensity units, respectively (difference not significant at 5% level). Puff amplitudes followed a Gaussian distribution (Fig. 8*B*), and similar distributions were observed from five other puff sites.

How much Ca^{2+} is released during a puff?

Because oocytes were loaded to a cytosolic concentration of about 40 μM calcium green-1, the estimate given above of the peak free Ca^{2+} change during a puff (140 nM) corresponds to binding of about 11·2 μM Ca^{2+} to dye molecules. In addition, Ca^{2+} would be bound to endogenous Ca^{2+} buffers in the oocyte. The extent of this is more difficult to estimate, but taking an endogenous buffering capacity between 10 and 100 (Allbritton *et al.* 1992; Zhou & Neher, 1993), a further 1·4–14 μM Ca^{2+} would be bound, giving a total cytosolic Ca^{2+} concentration (including that bound to dye, to endogenous buffers, and free in the cytosol) of between 12·8 and 25·4 μM. Since reuptake of Ca^{2+} is slow compared with the time to peak of the puff, we could neglect this factor and calculate the total amount of Ca^{2+} involved in a puff from the volume over which it was distributed. Estimates of this volume were made from two-dimensional images showing the lateral spread of Ca^{2+} at the peak of a puff by integrating the measured radial profile over three dimensions. The mean amount of Ca^{2+} in a puff derived in this way was $3–6 \times 10^{-18}$ mol (24 events analysed). Since this amount of Ca^{2+} was liberated during the roughly 50 ms rise time of a puff, the efflux rate was between about 6×10^{-17} and $1·2 \times 10^{-16}$ mol s^{-1}, depending upon values assumed for the endogenous buffering capacity. These rates correspond, respectively, to Ca^{2+} currents of about 11–23 pA.

Time distribution of Ca^{2+} puffs

Recordings of Ca^{2+} fluorescence showed that puffs occurred at irregular intervals at a given site (e.g. Fig. 8). However, the question arose whether their occurrence at a particular site was truly random, or followed a cyclical pattern. A random process, in which the occurrence of a puff is not influenced by preceding events, is expected to give rise to an exponential distribution of intervals between successive puffs, analogous to the time distribution of random miniature endplate potentials at the muscle endplate (Fatt & Katz, 1952). Alternatively, if Ca^{2+} release depended upon recovery from inactivation induced by a preceding Ca^{2+} release, the intervals between puffs should cluster around a certain mean interval.

Because the frequency of puffs was low, even at the most active sites, we were unable to collect sufficient events for satisfactory analysis during a continuous recording from a single puff site. Figure 9 therefore shows a distribution histogram of puff intervals obtained by pooling measurements from three puff sites in a single video record of 20 min duration, which showed similar mean puff frequencies. For interpuff intervals longer than about 10 s, the observed distribution matched well to an exponential curve with a time constant of about 14 s. However, at intervals shorter than 8 s, the number of observations declined progressively

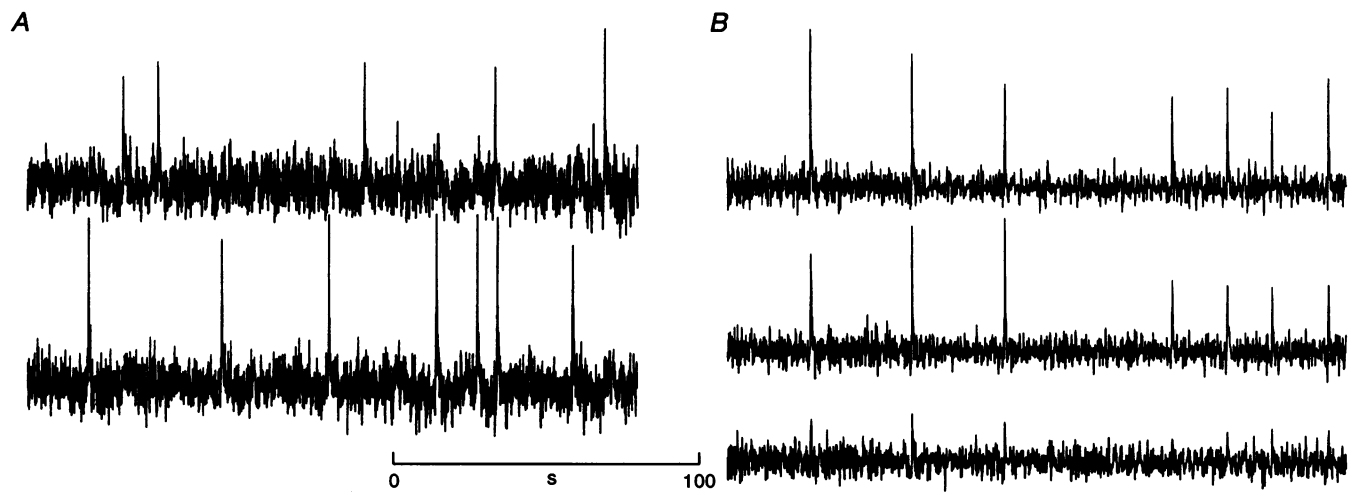

Figure 10. Asynchronous and synchronous activity from puff sites at different spacings

A, traces show puff activity recorded simultaneously from two sites 6·4 μm apart. Oocyte was loaded with 25 fmol 3-F-InsP_3. *B*, upper two traces show simultaneous records of puff activity at two sites 2·2 μm apart. The lower trace shows passive Ca^{2+} signals recorded simultaneously at a point 2·2 μm distant from both puff sites. Data are from a different oocyte to that in *A*.

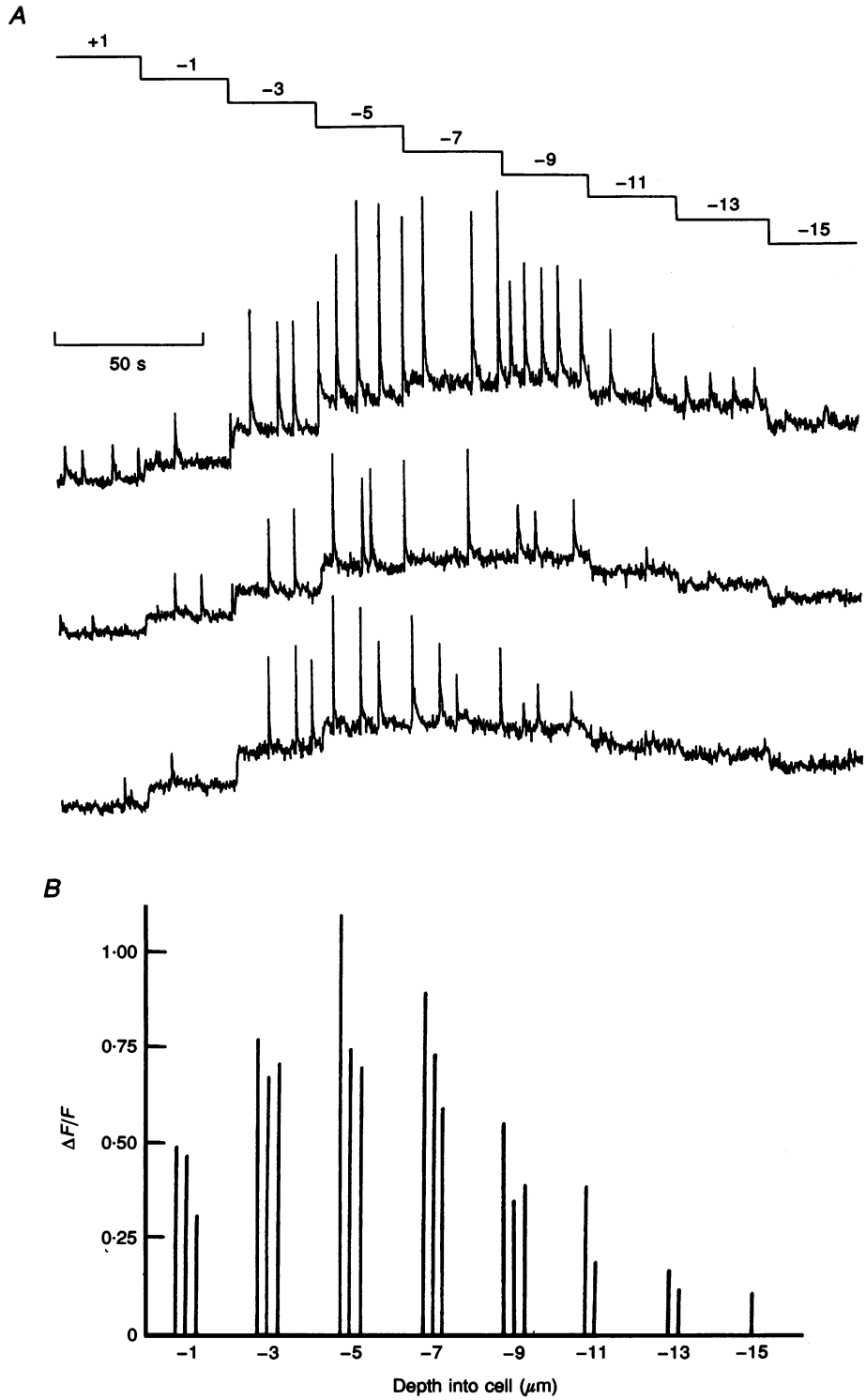

Figure 11. Puffs originate from Ca^{2+} release at sites about 5 μm below the cell membrane

A, simultaneous records of Ca^{2+} puffs monitored from 3 puff sites as the microscope focused in a stepwise fashion into the oocyte. Upper trace indicates the position (in μm) of the confocal optical section relative to the estimated boundary of the oocyte. *B*, peak size of Ca^{2+} puffs as a function of depth of the confocal section in the cell. Bars represent the peak puff amplitude at each depth monitored from the three sites in *A*, and are expressed as fractional increases in fluorescence above the resting fluorescence at corresponding depths ($\Delta F/F$).

(Fig. 9*B*), rather than continuing to increase. Thus, two factors appear to determine the interpuff interval. For several seconds following a puff the site may be refractory due to Ca^{2+}-dependent inhibition of $InsP_3$ receptors (Parker & Ivorra, 1990*b*; Bezprozvanny, Watras & Erlich, 1991), so that the probability of observing a second puff increases to a maximum after about 9 s as the inhibition decays. At longer times thereafter, the probability of observing a second puff decreases exponentially, suggesting that triggering of puffs is a random occurrence.

Autonomous and synchronized puffs from sites at different spacings

Simultaneous records of activity from puff sites spaced more than about 6 μm apart showed no obvious correlation (Fig. 10*A*), and this conclusion was confirmed by statistical analysis of recordings at three pairs of puff sites spaced about 7 μm apart. Thus, different sites can function autonomously, consistent with the idea that puffs may be triggered stochastically, and indicating that there are no factors (e.g. fluctuations of $InsP_3$ level or voltage across the membrane of the endoplasmic reticulum) that tend to synchronize activity over wide areas of the cell.

Different to this, recordings of puffs from more closely adjacent sites were highly correlated. For example, the upper two traces in Fig. 10*B* show recordings from two sites 2·2 μm apart, where the appearance of a puff at one site was invariably accompanied by a puff at the other site. This result could not be explained simply because the fluorescence recording at one site detected passive diffusion of Ca^{2+} from the other site, because control recordings (lower trace) at a point 2·2 μm from both puff sites showed only small signals. Instead, it seems that Ca^{2+} ions diffusing from a puff were able to trigger Ca^{2+} release from a closely adjacent site.

Depth of puff release sites in the oocyte

Puffs were most clearly resolved if the plane of the confocal section was focused a few micrometres below the surface of the oocyte, whereas at more superficial and deeper locations the Ca^{2+} signals were fainter and more diffuse. It thus seemed likely that the sites of Ca^{2+} release lay about 5 μm into the cell, so that rapid Ca^{2+} liberation from highly localized sources gave sharp Ca^{2+} signals at this depth, but that the signals recorded at other levels were attenuated and blurred by diffusion of Ca^{2+} ions.

Recordings of puff amplitudes are shown in Fig. 11*A*, monitored simultaneously from three puff sites as the microscope was focused in steps into the oocyte. At all sites, the largest signals were obtained at depths of 5–7 μm, and the puff amplitude declined above and below this level. However, a complication is that the amplitude of the fluorescence signals depends not only on the free Ca^{2+} change, but also on the amount of indicator dye sensed by the confocal spot and by absorption and scattering of light during its passage through the cell. To correct for these

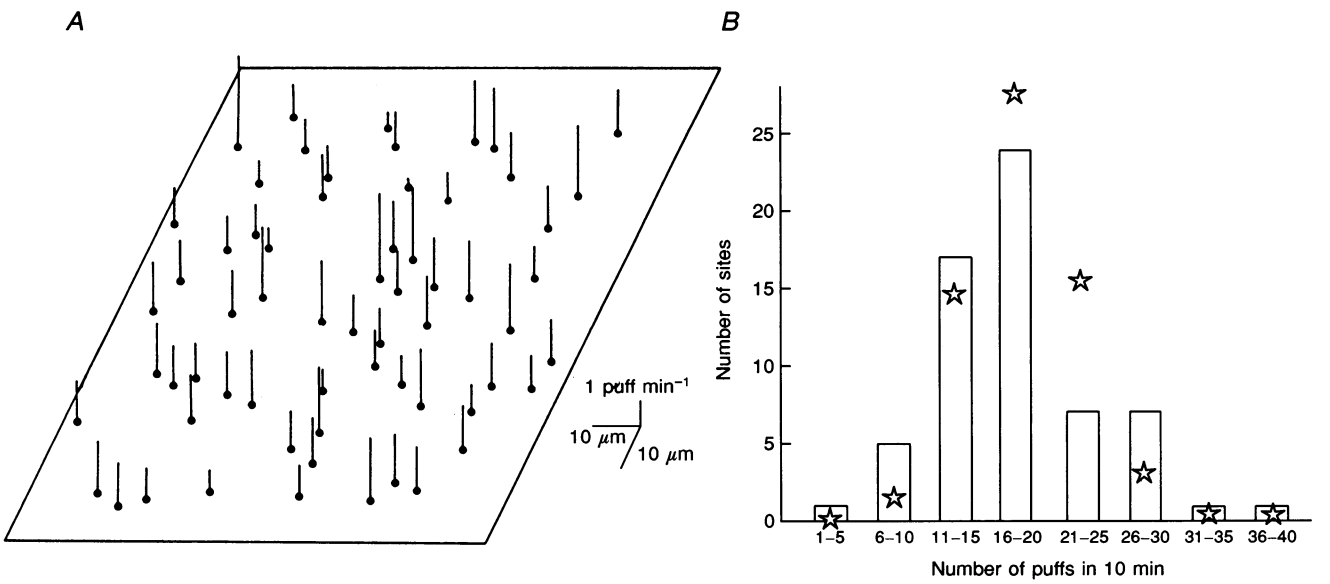

Figure 12. Lateral distribution of puff sites and distribution of puff frequencies at different sites

A, diagram represents a 100 × 100 μm region of an oocyte loaded with 35 fmol 3-F-$InsP_3$. Dots indicate sites where one or more puffs were observed during a 10 min recording period, and the heights of vertical bars represent the frequency of puffs at each site. *B*, measurements of puff frequencies obtained from the 64 puff sites illustrated in *A*. Histogram bars indicate the numbers of sites which showed a particular number of puffs during the 10 min recording period. Stars indicate the Poisson distribution expected if the probability of occurrence of puffs was equal at all sites. The mean puff frequency was 1·84 min^{-1}.

latter influences, we expressed peak fluorescence signals during puffs as a fractional change over the resting fluorescence value at each depth ($\Delta F/F$) (Fig. 11*B*). This normalized measure also indicated that free Ca^{2+} levels during puffs were greatest at a depth of about 5 μm into the cell.

Lateral distribution of puff sites

To examine the lateral distribution of puffs across the oocyte surface we repeatedly replayed video records of puff activity, and marked on an acetate sheet affixed to the video monitor the number of puffs observed at each site during a fixed recording period. Figure 12*A* shows measurements from a 100 × 100 μm region of an oocyte, in which puff sites are identified by dots, and vertical bars indicate the number of puffs observed at each site during a 10 min recording period.

An estimate of the mean density of puff sites was obtained by counting the numbers of sites within 10 × 10 μm

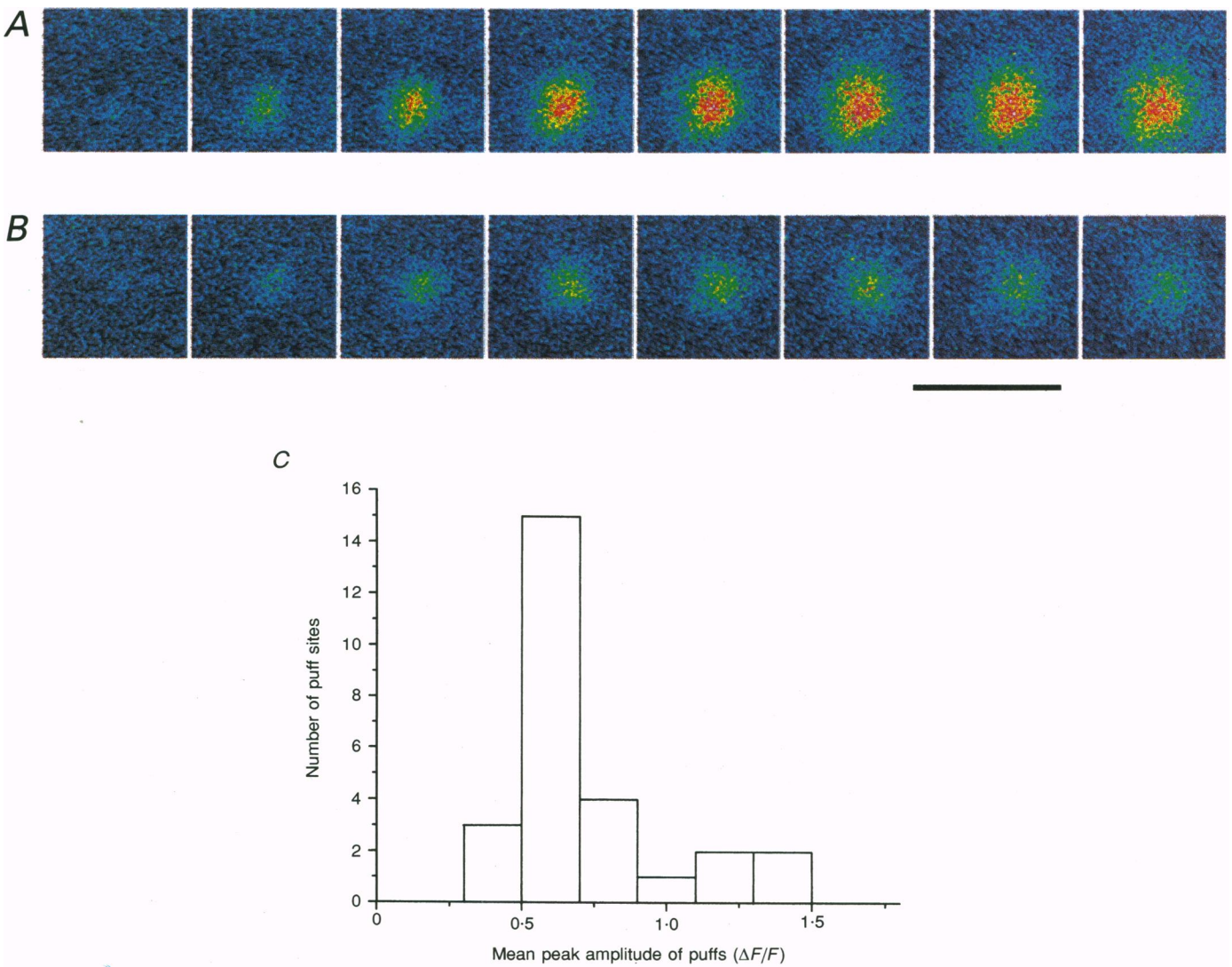

Figure 13. Ca^{2+} release sites showing 'giant' and 'normal' sized puffs

A and *B*, image sequences show the time course of puffs generated at two sites about 12 μm apart which showed, respectively, giant and normal puffs. Sequential frames are shown at intervals of 16·6 ms, and increasingly 'warm' colours depict increasing Ca^{2+}-dependent fluorescence. The data were not calibrated in terms of absolute free Ca^{2+} concentration, but all images were processed identically, so that any given fractional change in fluorescence intensity ($\Delta F/F$) corresponds to the same colour. Images in *A* are an average of 10 puffs at a single site giving large signals, and images in *B* are an average of 6 puffs from an adjacent site in the same video recording. Scale bar, 10 μm. *C*, distribution of mean puff amplitudes at different puff sites. The histogram was derived from measurements of fluorescence signals at 27 puff sites from 3 recording areas. Measurements were made of peak fluorescence signals during 3 puffs at each site, and the bars indicate the numbers of sites showing various fractional fluorescence changes ($\Delta F/F$).

squares that showed at least one puff during a 5 min period. The mean value from seventy-five monitoring squares positioned on the animal hemispheres of three oocytes was $3{\cdot}3 \pm 0{\cdot}6$. Thus, the average density of puff sites was about 1 per 30 μm^2.

Variation in puff frequency between different sites

It is apparent from Fig. 12*A* that the numbers of puffs varied appreciably between different sites. To see whether this arose from differences in sensitivities between sites, or whether it simply reflected statistical variation, we measured the distribution of puff occurrences. Figure 12*B* plots the numbers of sites which showed various numbers of puffs during the 10 min recording period. If all sites were to show an equal probability of giving a puff, the distribution of observed numbers of puffs per site would be expected to follow a Poisson distribution. The stars in Fig. 12*B* indicate the distribution predicted from the observed mean puff frequency (18·4 puffs per 10 min). This provided a reasonably good fit to the data, suggesting that most of the variability in puff frequency between different sites arises through statistical fluctuations, and that different sites show similar sensitivities to $InsP_3$.

Variability in puff amplitude between different sites

As described above, puffs produced at a given site tended to be of similar amplitude. However, it was obvious when viewing the video recordings that a few sites consistently produced puffs that were larger than at neighbouring sites. An example is shown in Fig. 13*A* and *B*, which shows images averaged from several puff events at two adjacent sites that showed, respectively, 'giant' and 'normal' sized puffs. The mean fluorescence change ($\Delta F/F$) at the site shown in *A* was $1{\cdot}41 \pm 0{\cdot}10$ (10 puffs) as compared with $0{\cdot}50 \pm 0{\cdot}04$ (6 puffs) at the site shown in *B* (difference significant at 0·1 % level by Student's *t* test). However, the time to peak was similar for puffs at the two sites (Fig. 13*A* and *B*), indicating that the greater fluorescence signal at the site shown in *A* did not result because Ca^{2+} liberation persisted for longer, but instead must have arisen because of a greater Ca^{2+} flux. Also, Ca^{2+} became elevated over a greater area during the giant puff, and the fluorescence signal decayed more slowly.

Figure 13*C* shows the distribution of mean puff amplitudes measured from twenty-seven sites. Most sites showed a narrow range of fluorescence signals, clustered around a mean $\Delta F/F$ of about 0·6, but a few sites (4 of the 27) showed considerably greater signals, with a $\Delta F/F$ greater than 1·1. Furthermore, comparison of the fluorescence signals appreciably underestimates the difference in free Ca^{2+} levels during normal and giant puffs, since the dye signal approached saturation at the peak of giant puffs. For example, the peak free Ca^{2+} levels during the puffs in Fig. 13*A* and *B* were estimated to be, respectively, about 1·5 μM and 200 nM (assuming values derived in other oocytes of resting free Ca^{2+} level = 40 nM and $F_{max}/F_{min} = 3{\cdot}9$).

Except for Fig. 13 all data in this paper were derived from sites giving puffs of 'normal' size (i.e. peak $\Delta F/F$ of about 0·5).

DISCUSSION

Our results show that low concentrations of $InsP_3$ evoke transient, localized elevations of cytosolic Ca^{2+} in *Xenopus* oocytes, which last a few hundred milliseconds and are restricted to within a few micrometres. The amplitudes of these puffs show a roughly all-or-none characteristic, whereas their frequency increases steeply with an increasing concentration of $InsP_3$. Thus, Ca^{2+} puffs appear to represent a basic 'quantal unit' of $InsP_3$-mediated Ca^{2+} liberation. Their importance for cell functioning may lie in the fact that puffs can act as foci to trigger propagating Ca^{2+} waves when levels of $InsP_3$ (Parker & Yao, 1991) or intracellular free Ca^{2+} (Yao & Parker, 1994) are elevated.

Localized, quantal Ca^{2+} mobilization by $InsP_3$ appears not to be peculiar to the oocyte, but may be a general feature of $InsP_3$ signalling in other cell types. For example, two recent reports (Thorn, Lawrie, Smith, Gallacher & Petersen, 1993; Kasai, Li & Miyashita, 1993) describe localized Ca^{2+} spikes in pancreatic acinar cells, and spontaneous Ca^{2+}-activated currents (STOCs) in smooth muscle cells are likely to result from quantal release of Ca^{2+} from $InsP_3$-sensitive intracellular stores (Komori & Bolton, 1991). More surprisingly, an analogous quantal characteristic is seen with Ca^{2+} release from sarcoplasmic reticulum mediated through ryanodine receptor–channels. Cheng, Lederer & Cannell (1993) describe transient, localized calcium 'sparks' in cardiac muscle, which increase in frequency and become able to trigger propagating Ca^{2+} waves when stimulated by low concentrations of ryanodine.

Quantal nature of Ca^{2+} liberation by $InsP_3$

The appearance of puffs demonstrates that $InsP_3$-mediated Ca^{2+} liberation in the oocyte shows quantal characteristics, in the sense that Ca^{2+} is released in a nearly all-or-none manner from multiple discrete and autonomous stores within the cell. However, the term 'quantal' release was first used in the context of $InsP_3$-induced Ca^{2+} liberation to describe a quite different phenomenon, namely the finding that sub-optimal concentrations of $InsP_3$ lead to the rapid release of only a fraction of the total releasable Ca^{2+} from populations of permeabilized cells (Muallem, Pandol & Beeker, 1989; Taylor & Potter, 1990; Meyer & Stryer, 1990). One explanation proposed to account for this incremental release characteristic is that $InsP_3$-sensitive stores are arranged as autonomous quantal units, which release their contents in an all-or-none manner at varying threshold concentrations of $InsP_3$ (Muallem *et al.* 1989; Taylor & Potter, 1990). Thus, a low concentration of $InsP_3$ may evoke complete release from a population of highly sensitive stores, whereas other, less sensitive, stores would release their contents only at higher concentrations of $InsP_3$. A different proposal is that $InsP_3$ receptors show an

adaptive characteristic (Gyorke & Fill, 1993), or are modulated by intraluminal Ca^{2+} (Missiaen, Taylor & Berridge, 1992), so that each store releases only a certain fraction of its contents in the sustained presence of a particular concentration of $InsP_3$.

At first sight, our results might seem to support the notion that the incremental release of Ca^{2+} in response to increasing $InsP_3$ concentrations arises from the quantal organization of $InsP_3$-sensitive Ca^{2+} stores. However, a key point of that idea is that the stores must be heterogeneous, with widely differing sensitivities to $InsP_3$. Against this, we found little evidence for differing sensitivities of sites giving rise to Ca^{2+} puffs. Furthermore, once the $InsP_3$ concentration exceeded a certain level, Ca^{2+} waves were triggered and spread across the oocyte to recruit release from other stores in the cell in an abrupt all-or-none manner, rather than in a continuous, incremental fashion. Also, we failed to observe any adaptation of $InsP_3$-evoked Ca^{2+} liberation which might account for the incremental characteristic, since puffs were generated at roughly constant frequency for as long as 30 min in the presence of a fixed concentration of 3-F-$InsP_3$.

Mechanisms giving rise to the puff

The Ca^{2+} puffs evoked by $InsP_3$ show several well-defined characteristics: they are nearly all-or-none events that remain highly localized within the cell and occur stochastically at a frequency that increases as about the third power of the $InsP_3$ concentration. How might these properties be explained?

An intriguing possibility is that the all-or-none characteristic might arise because a puff results from the opening of a single $InsP_3$ receptor–channel molecule. Such a mechanism has been proposed to explain the Ca^{2+} sparks seen in heart muscle (Cheng *et al.* 1993), though calculations based on our data indicate that the amount of Ca^{2+} released during a puff is probably too large to be reasonably explained by flux through a single channel. Ca^{2+} efflux during a puff was estimated to occur at a rate corresponding to an ionic current of between 11 and 23 pA. Single $InsP_3$-receptor channels, purified from oocyte membranes and reconstituted in lipid bilayers, show a maximal current of only about 1 pA with 50 mM Ca^{2+} as the charge carrier and a 30 mV electrical driving force (N. Callamaras; unpublished data). It is difficult to estimate what current would pass through a channel in the intact cell, since we know neither the intraluminal Ca^{2+} concentration nor the voltage across the membrane of the Ca^{2+} stores. Nevertheless, it seems unlikely from these numbers that Ca^{2+} efflux through a single channel could account for a puff, but rather that a puff results from the concerted opening of several channels in close proximity. The variability in sizes of puffs evoked at different sites may also be consistent with this idea, if the numbers of channels clustered at each site vary. However, because estimates of the amount of Ca^{2+} in a puff, and of the ionic flux through single $InsP_3$-gated channels, are subject to considerable errors, we cannot entirely rule out the possibility that a puff arises from opening a single channel. A good test of this idea would be to load oocytes with increasing concentrations of an irreversible $InsP_3$ antagonist, and observe whether sites become knocked out in an all-or-none manner, or whether puff amplitudes progressively diminish. Unfortunately, an appropriate antagonist is not yet available.

One conclusion that can be drawn with some certainty is that puffs cannot result from stochastic openings of single channels, since the open-time distribution is then expected to be exponentially distributed (Hille, 1992). Because the amplitude of a puff reflects the total charge carried by Ca^{2+} (current × time), we expect that if puffs result from single channel openings, their amplitudes should be exponentially distributed, with many small puffs and progressively fewer larger puffs. This was not observed. Instead, the amplitudes of puffs at a given site were distributed in a Gaussian manner around a mean value.

An explanation for this result may be that the duration of a channel opening or burst of openings is determined not stochastically, but rather by feedback processes contingent on release of Ca^{2+} into the cytosol. Such a mechanism would be equally applicable regardless of whether a puff involves opening of a single channel, or a number of channels clustered together at a spacing small compared with the diffusion coefficient for Ca^{2+}. For example, positive feedback by moderate levels of cytosolic Ca^{2+} during the rising phase of a puff may increase the opening probability of the channel, whereas the higher Ca^{2+} level at the peak of a puff may inhibit channel opening and thus terminate Ca^{2+} release (Parker & Ivorra, 1990*b*; Finch, Turner & Goldin 1991; Bezprozvanny *et al.* 1991; Iino & Endo, 1992; Yao & Parker, 1992). Puffs would be of roughly constant size, because the duration of Ca^{2+} liberation is determined by the average kinetics of thousands of Ca^{2+} ions as they accumulate in the cytosol, rather than the stochastic behaviour of a single receptor–channel molecule.

The nature of the positive feedback by cytosolic Ca^{2+} ions on $InsP_3$-evoked Ca^{2+} release is a matter of some controversy, and has been proposed to arise either because Ca^{2+}-mediated stimulation of phospholipase C results in increased formation of endogenous $InsP_3$ (Harootunian, Kao, Paranjape, Adams, Potter & Tsien, 1991), or because Ca^{2+} acts as a co-agonist at the $InsP_3$ receptor (Bezprozvanny *et al.* 1991; Finch *et al.* 1991). We have previously presented evidence favouring the latter model in the oocyte (Parker & Yao, 1991; Yao & Parker, 1992; Parker & Ivorra, 1993), and the characteristics of the puffs further suggest that their rapid upstroke is unlikely to result through feedback via phospholipase C. Firstly, the duration of Ca^{2+} release during a puff (about 50 ms) is short compared with the time for Ca^{2+} ions to diffuse to the plasma membrane from a puff site at a depth of several micrometres into the cell. Secondly, if $InsP_3$ were to be

formed during a puff, it would be expected to diffuse more rapidly than Ca^{2+} ions (Allbritton *et al.* 1992), and perhaps to evoke Ca^{2+} release from sites surrounding the original puff.

Following a relative refractory period of a few seconds, the occurrence of puffs at a given site was random, and the frequency of puffs increased as about the third power of 3-F-InsP_3 concentration. This power relation indicates a co-operative action of InsP_3 molecules in triggering puffs, but it is not clear whether this results from co-operativity at a single receptor molecule or between several InsP_3 receptor–channels. For example, if the stochastic opening of a single channel were sufficient to trigger a puff, co-operativity may arise if channel opening requires simultaneous binding of three or more InsP_3 molecules to sites on the tetrameric InsP_3 receptor (Meyer, Holowka & Stryer, 1988). Alternatively, the amount of Ca^{2+} passing through a single channel may be insufficient to trigger a puff, and instead the near-simultaneous opening of several adjacent channels may be needed to provide sufficient Ca^{2+} to evoke regenerative feedback.

Spatial organization of puff sites

Ca^{2+} puffs arose from Ca^{2+} released at sites restricted to a narrow layer about 5 μm deep into the cell. This is consistent with immunolocalization studies showing that InsP_3 receptors in the oocyte are concentrated in a narrow, subplasmalemmal band (Parys, Sernett, DeLisle, Snyder, Welsh & Campbell, 1992; Kume *et al.* 1993; Callamaras & Parker, 1994).

The lateral distribution of puffs indicated that release sites are present at a density of about 1 per 30 μm^2, giving a rough estimate of about 100 000 puff sites per oocyte (1 mm diameter). This figure is, therefore, also a minimal estimate of the number of InsP_3 receptors present in an oocyte, and the number would increase to 1 million if each puff site comprises a cluster of about ten receptor–channels. Further, immunolocalization studies reveal a diffuse staining throughout the bulk of the cell and more intensely around the nuclear envelope (Callamaras & Parker, 1994), indicating the presence of InsP_3 receptors in addition to those involved in the puffs.

The excitable medium in which Ca^{2+} waves propagate in the oocyte may, therefore, be considered as a two-dimensional sheet a few micrometres below the cell surface, which is formed by functionally discrete InsP_3-sensitive Ca^{2+} stores distributed at an average spacing of about 6 μm. This granularity of release sites is relatively coarse as compared with the space constant of Ca^{2+} ions released during a puff (2·8 μm), and may explain why puffs remain localized. At concentrations of InsP_3-evoking puffs, the cytosolic Ca^{2+} concentration at a puff site presumably rises sufficiently high to allow a local regenerative feedback resulting in an all-or-none Ca^{2+} release (Yao & Parker, 1992; Parker & Ivorra, 1993). However, the diffusional spread of Ca^{2+} from one site may be inadequate to evoke regenerative release from neighbouring sites. Only when the concentration of InsP_3 is raised further do surrounding sites become sufficiently sensitive that Ca^{2+} ions diffusing from an initial focus are able to trigger regenerative release, which, in turn, triggers yet further sites resulting in a propagating wave. The spatial organization of Ca^{2+} release sites is, therefore, likely to be of crucial importance in determining whether Ca^{2+} waves are able to propagate, and further suggests that wave propagation will occur in a saltatory manner. Such considerations have not yet been taken into account in attempts to model Ca^{2+} wave propagation (e.g. Atri *et al.* 1993), where the Ca^{2+} stores have generally been assumed to form a homogeneous medium.

Allbritton, N. L., Meyer, T. & Stryer, L. (1992). Range of messenger action of calcium ion and inositol 1,4,5-trisphosphate. *Science* **258**, 1812–1815.

Atri, A., Amundson, J., Clapham, D. & Sneyd, J. (1993). A single-pool model for intracellular calcium oscillations and waves in the *Xenopus laevis* oocyte. *Biophysical Journal* **65**, 1727–1739.

Berridge, M. J. (1988). Inositol trisphosphate-induced membrane current oscillations in *Xenopus* oocyte. *Journal of Physiology* **403**, 589–599.

Berridge, M. J. (1993). Inositol trisphosphate and calcium signalling. *Nature* **361**, 315–325.

Bezprozvanny, I., Watras, J. & Erlich, B. E. (1991). Bell-shaped calcium-response curves of Ins(1,4,5)P_3- and calcium-gated channels from endoplasmic reticulum of cerebellum. *Nature* **351**, 751–754.

Callamaras, N. & Parker, I. (1994). Inositol 1,4,5-trisphosphate receptors in *Xenopus laevis* oocytes: localization and modulation by Ca^{2+}. *Cell Calcium* **15**, 60–72.

Cheng, H., Lederer, W. J. & Cannell, M. B. (1993). Calcium sparks: elementary events underlying excitation–contraction coupling in heart muscle. *Science* **262**, 740–744.

Crank, J. (1975). *The Mathematics of Diffusion*, pp. 28–29. Clarendon Press, Oxford.

Eberhard, M. & Erne, P. (1991). Calcium binding to fluorescent calcium indicators: calcium green, calcium orange and calcium crimson. *Biochemical and Biophysical Research Communications* **180**, 209–215.

Fatt, P. & Katz, B. (1952). Spontaneous subthreshold activity at motor nerve endings. *Journal of Physiology* **117**, 109–128.

Finch, E. A., Turner, T. J. & Goldin, S. M. (1991). Calcium as a coagonist of inositol 1,4,5-trisphosphate-induced calcium release. *Science* **254**, 443–446.

Gyorke, S. & Fill, M. (1993). Ryanodine receptor adaptation: control mechanism of Ca^{2+}-induced Ca^{2+} release in heart? *Science* **260**, 807–809.

Harootunian, A. T., Kao, J. P. Y., Paranjape, S., Adams, S. R., Potter, B. L. V. & Tsien, R. Y. (1991). Cytosolic Ca^{2+} oscillations in REF52 fibroblasts: Ca^{2+}-stimulated IP_3 production or voltage-dependent Ca^{2+} channels as key positive feedback elements. *Cell Calcium* **12**, 153–164.

HILLE, B. (1992). *Ionic Channels of Excitable Membranes.* Sinauer Associates, Sunderland, MA, USA.

IINO, M. & ENDO, M. (1992). Calcium-dependent immediate feedback control of inositol 1,4,5-trisphosphate-induced Ca^{2+} release. *Nature* **360**, 76–78.

KASAI, H., LI, Y. X. & MIYASHITA, Y. (1993). Subcellular distribution of Ca^{2+} release channels underlying Ca^{2+} waves and oscillations in exocrine pancreas. *Cell* **74**, 669–677.

KOMORI, S. & BOLTON, T. B. (1991). Calcium release induced by inositol 1,4,5-trisphosphate in single rabbit intestinal smooth muscle cells. *Journal of Physiology* **433**, 495–517.

KOZIKOWSKI, A. P., FAUQ, A. H., ASKOY, I. A., SEEWALD, M. J. & POWIS, G. (1990). Synthesis of the first optically pure, fluorinated inositol 1,4,5-trisphosphate of *myo*-inositol. Stereochemistry and its effect on Ca^{2+} release in Swiss 3T3 cells. *Journal of the American Chemical Society* **112**, 7403–7404.

KUME, S., MUTO, A., ARUGA, J., NAKAGAWA, T., MICHIKAWA, T., FURUICHI, T., NAKADE, S., OKANO, H. & MIKOSHIBA, K. (1993). The *Xenopus* IP_3 receptor: structure, function, and localization in oocytes and eggs. *Cell* **73**, 555–570.

LECHLEITER, J. D. & CLAPHAM, D. E. (1992). Molecular mechanisms of intracellular calcium excitability in X. laevis oocytes. *Cell* **69**, 283–294.

LECHLEITER, J. D., GIRARD, S., PERALTA, E. & CLAPHAM, D. E. (1991). Spiral calcium wave propagation and annihilation in *Xenopus laevis* oocytes. *Science* **252**, 123–126.

MCCRAY, J. A. & TRENTHAM, D. R. (1989). Properties and uses of photoreactive caged compounds. *Annual Review of Biophysics and Biophysical Chemistry* **18**, 239–270.

MEYER, T. (1991). Cell signalling by second messenger waves. *Cell* **64**, 675–678.

MEYER, T., HOLOWKA, D. & STRYER, L. (1988). Highly cooperative opening of calcium channels by inositol 1,4,5-trisphosphate. *Science* **240**, 653–656.

MEYER, T. & STRYER, L. (1990). Transient calcium release induced by successive increments of inositol 1,4,5-trisphosphate. *Science* **240**, 653–656.

MEYER, T. & STRYER, L. (1991). Calcium spiking. *Annual Review of Biophysics and Biophysical Chemistry* **18**, 239–270.

MISSIAEN, L., TAYLOR, C. W. & BERRIDGE, M. J. (1992). Luminal Ca^{2+} promoting spontaneous Ca^{2+} release from inositol trisphosphate-sensitive stores in rat hepatocytes. *Journal of Physiology* **455**, 623–640.

MUALLEM, S., PANDOL, S. J. & BEEKER, T. G. (1989). Hormone-evoked calcium release from intracellular stores is a quantal process. *Journal of Biological Chemistry* **264**, 205–212.

PARKER, I. (1992). Caged intracellular messengers and the inositol phosphate pathway. In *Neuromethods*, vol. 20, *Intracellular Messengers*, ed. BOULTON, A., BAKER, G. B. & TAYLOR, C., pp. 369–393. Humana Press, New Jersey.

PARKER, I. & IVORRA, I. (1990*a*). Localized all-or-none calcium liberation by inositol trisphosphate. *Science* **250**, 977–979.

PARKER, I. & IVORRA, I. (1990*b*). Inhibition by Ca^{2+} of inositol trisphosphate-mediated Ca^{2+} liberation: a possible mechanism for oscillatory release of Ca^{2+}. *Proceedings of the National Academy of Sciences of the USA* **87**, 260–264.

PARKER, I. & IVORRA, I. (1992). Characteristics of membrane currents evoked by photorelease of inositol trisphosphate in *Xenopus* oocytes. *American Journal of Physiology* **263**, C154–165.

PARKER, I. & IVORRA, I. (1993). Confocal microfluorimetry of Ca^{2+} signals evoked in *Xenopus* oocytes by photoreleased inositol trisphosphate. *Journal of Physiology* **461**, 133–165.

PARKER, I. & YAO, Y. (1991). Regenerative release of calcium from functionally discrete subcellular stores by inositol trisphosphate. *Proceedings of the Royal Society* B **246**, 269–274.

PARYS, J. B., SERNETT, S. W., DELISLE, S., SNYDER, P. M., WELSH, M. J. & CAMPBELL, K. P. (1992). Isolation, characterization, and localization of the inositol 1,4,5-trisphosphate receptor protein in *Xenopus laevis* oocytes. *Journal of Biological Chemistry* **267**, 18776–18782.

SUMIKAWA, K., PARKER, I. & MILEDI, R. (1989). Expression of neurotransmitter receptors and voltage-activated channels from brain mRNA in *Xenopus* oocytes. *Methods in Neurosciences* **1**, 30–45.

TAYLOR, C. W. & POTTER, B. V. L. (1990). The size of inositol 1,4,5-trisphosphate sensitive stores depends on inositol 1,4,5-trisphosphate concentration. *Biochemical Journal* **266**, 189–194.

THORN, P., LAWRIE, A. M., SMITH, P. M., GALLAGHER, D. V. & PETERSEN, O. H. (1993). Local and global cytosolic Ca^{2+} oscillations in exocrine cells evoked by agonists and inositol trisphosphate. *Cell* **74**, 661–668.

TIGYI, G. & MILEDI, R. (1992). Lysophosphatidates bound to serum albumin activate membrane currents in *Xenopus* oocytes and cause neurite retraction in PC12 pheochromocytoma cells. *Journal of Biological Chemistry* **267**, 21360–21367.

YAO, Y. & PARKER, I. (1992). Potentiation of inositol trisphosphate-induced Ca^{2+} mobilization in *Xenopus* oocytes by cytosolic Ca^{2+}. *Journal of Physiology* **458**, 319–338.

YAO, Y. & PARKER, I. (1993). Inositol trisphosphate-mediated Ca^{2+} influx into *Xenopus* oocytes triggers Ca^{2+} liberation from intracellular stores. *Journal of Physiology* **468**, 275–296.

YAO, Y. & PARKER, I. (1994). Ca^{2+} influx modulation of temporal and spatial patterns of inositol trisphosphate-mediated Ca^{2+} liberation in *Xenopus* oocytes. *Journal of Physiology* **476**, 17–28.

ZHOU, Z. & NEHER, E. (1993). Mobile and immobile calcium buffers in bovine adrenal chromaffin cells. *Journal of Physiology* **469**, 245–273.

Acknowledgements

This work was supported by grant GM48071 from the US Public Health Service.

Received 2 February 1994; accepted 11 July 1994.